International Journal of Advanced Technology and Engineering Exploration, Vol 12(126)
ISSN (Print): 2394-5443 ISSN (Online): 2394-7454
http://dx.doi.org/10.19101/IJATEE.2023.10102484

Research Article

Electromagnetic vector PSO technique for combined economic and emission dispatch

Nilanjan Mitra*, Saroja Kumar Dash and Himanshu Shekhar Maharana
Department of Electrical Engineering, GITA, Autonomous College, Bhubaneswar, Affiliated to Biju Patnaik University of Technology, Rourkela, Odisha, India

Received: 10-June-2023; Revised: 28-March-2025; Accepted: 09-May-2025

Abstract
Economic dispatch optimization problems with convex or quasi-convex characteristics, subject to equality and inequality constraints, are challenging due to their inherent non-linear nature. These complexities arise from factors such as fuel type, transmission system ramp rate limits, valve point effects, cost fluctuations, and valve point loading (VPL). This paper presents an electromagnetic vector particle swarm optimization (EVPSO) technique to address a range of complex and semi-economic load dispatch problems across different power systems. The method incorporates a phasor-based mechanism to enhance standard particle swarm optimization (PSO) control structures. EVPSO is applied to three system configurations involving fifteen, forty, and one hundred generating units, considering transmission losses without imposing ramp rate constraints. Comparative simulations demonstrate that EVPSO performs effectively, emerging as a reliable approach capable of delivering high-quality solutions for various economic load dispatch (ELD) scenarios. The technique consistently yields promising results across different system sizes and configurations, surpassing conventional methods in handling non-linearities and operational constraints. The development of EVPSO represents a significant advancement in solving complex optimization problems in economic dispatch, highlighting its potential as a robust tool for achieving efficient and dependable energy dispatch across diverse power system environments.

Keywords
Economic load dispatch, Electromagnetic vector particle swarm optimization (EVPSO), Non-linear optimization, Power system operation, Valve point loading.

1.Introduction
The growing need for environmentally sustainable and cost-effective energy management strategies has accelerated the development of advanced optimization methods tailored for modern power systems. Among the critical challenges, the combined economic and emission dispatch (CEED) problem [1] stands out due to its dual objective—minimizing both fuel cost and pollutant emissions. However, CEED is characterized by its nonlinear, non-convex, and multimodal nature, which renders conventional optimization techniques inadequate in achieving optimal or near-optimal solutions.

To overcome these complexities, researchers have adopted nature-inspired metaheuristic algorithms such as differential evolution (DE) [2], evolutionary programming (EP) [3], genetic algorithms (GA) [4], and Biogeography-Based Optimization (BBO) [5]. These algorithms offer flexibility and robustness in navigating non-convex landscapes. Among them, particle swarm optimization (PSO) [6] has gained considerable attention for its balance between exploration and exploitation. However, conventional PSO often suffers from early convergence and stagnation in local optima, limiting its effectiveness in solving CEED.

To address these limitations, electromagnetic-inspired particle swarm optimization (EVPSO) has emerged as a promising solution [7, 8]. EVPSO extends PSO by introducing mechanisms inspired by electromagnetic field theory, allowing particles to attract or repel one another, thus maintaining diversity in the swarm and improving global search capabilities. The EVPSO algorithm iteratively refines particle positions in the multivariate search space, enhancing both convergence speed and solution quality compared to classical methods [9, 10].

*Author for correspondence

The motivation for this study stems from the need for more adaptive and robust optimization techniques to tackle CEED, particularly in the context of increasing global concerns about environmental degradation and climate change. Minimizing emissions from power generation has become a regulatory and ethical necessity. Hence, optimization methods must not only ensure economic feasibility but also support environmental sustainability [11].

This research seeks to fill the gaps in existing methods by introducing an advanced EVPSO framework that improves the exploration-exploitation trade-off, mitigates premature convergence, and performs reliably across complex CEED landscapes. The algorithm is tested on standard CEED benchmark problems to demonstrate its effectiveness relative to other optimization techniques such as DE, EP, GA, and hybrid PSO approaches [12–14].

Furthermore, the practical significance of EVPSO lies in its potential for deployment in real-world systems, where uncertainty, dynamic load demand, and emission constraints must be accounted for. This makes EVPSO not only a theoretical contribution but also a viable candidate for application in sustainable power system operation [15–20].

This study aims to develop and evaluate the EVPSO method to address the challenges of CEED. The primary objective is to simultaneously minimize power generation costs and pollutant emissions by improving the exploration and exploitation capabilities of the optimization process. The proposed EVPSO framework integrates electromagnetic principles into the conventional PSO algorithm to overcome issues such as premature convergence and limited solution diversity. By benchmarking the proposed method against established techniques such as DE, EP, GA, and hybrid PSO, the study highlights its superior performance in terms of solution quality and convergence speed. The research also contributes a detailed analysis of the trade-offs between economic and environmental objectives, offering valuable insights for real-world power system applications and decision-making processes.

The rest of the paper is organized as follows: literature review in Section 2, materials and method in Section 3, results and discussion in Section 4, and concluded in Section 5.

2.Literature review

The economic load dispatch (ELD) problem has been extensively explored, leading to the development of numerous optimization techniques aimed at enhancing power system performance. This literature review examines key methodologies applied to ELD, with a focus on multi-objective optimization, hybrid approaches, and recent algorithmic advancements. Han et al. introduced a multi-objective PSO technique with adaptive strategies, demonstrating its effectiveness in balancing exploration and exploitation [21]. Although PSO—modeled on social behavior—has been effective in handling ELD problems, it suffers from limitations such as early convergence and limited exploration capacity. Niknam et al. modified the teaching-learning-based optimization algorithm for reserve-constrained dynamic ELD, mimicking classroom-based teaching-learning processes to address dynamic constraints more effectively.

Hybrid approaches have gained prominence for their ability to integrate the strengths of multiple algorithms. Kavousi-fard and Akbari-zadeh proposed a hybrid framework using wavelet transforms, artificial neural networks (ANNs), and autoregressive integrated moving average (ARIMA) models for short-term load forecasting, improving both prediction accuracy and optimization efficiency. BBO, inspired by species migration patterns, has also been employed for economic emission dispatch due to its ability to maintain population diversity and avoid premature convergence [5]. Yang et al. [6] applied EP for economic dispatch and Sinha et al. [7] demonstrated EP's effectiveness in addressing complex fuel cost functions.

Recent developments have focused on hybrid metaheuristic strategies that enhance solution quality and convergence speed. Mason et al. and Ghasemi et al. proposed the multi-objective simulated annealing local search pattern swarm algorithm (MSSA) for dynamic economic emission dispatch (DEED) [22, 23], which integrates swarm intelligence with local search to handle dynamic characteristics of economic dispatch. Kaur et al. [24] developed a hybrid metaheuristic model combining heuristic optimization with deep learning-based forecasting for techno-economic dispatch in combined heat and power (CHP) systems, significantly improving microgrid management efficiency.

Hybrid methodologies have shown great promise by leveraging complementary algorithmic capabilities. However, they also introduce challenges such as increased computational complexity, which can hinder real-time implementation, particularly in large-scale systems. The effectiveness of such methods is highly dependent on the integration strategy and requires extensive tuning. Furthermore, hybrid metaheuristics [25, 26], though capable of producing high-quality solutions, often lack interpretability and may be difficult to deploy in operational contexts without a deep understanding of their internal mechanisms. Recent research has also emphasized specific sub-domains, such as CHP systems and emission-constrained dispatch [27, 28], providing valuable insights but sometimes lacking general applicability.

Future efforts should focus on the development of comprehensive optimization frameworks that simultaneously address multiple objectives and constraints [29]. Several recent studies have laid the groundwork for analyzing soft computing techniques, particularly the electromagnetic vector-based PSO (EVPSO) [30, 31]. Investigated CEED in CHP systems using direct solution techniques, while proposed a hybrid chaotic-based multi-objective DE model for economic emission dispatch, enhancing convergence and accuracy. Bhargava and Yadav introduced a hybrid DE and Crow Search Algorithm for CEED [32], and Habib et al. [29] applied the honey bee mating optimization (HBMO) method, addressing both cost and emission constraints.

Niknam et al. also extended MSSA for DEED [2], and proposed hybrid algorithms for CEED [33–35], reporting improved solution quality. Kaur et al. [24] integrated wind power with hybrid metaheuristic approaches in CHP dispatch systems [36, 37], further enhancing precision and operational efficiency. The literature on ELD optimization [38, 39] highlights significant progress in hybrid metaheuristic development, offering robust tools for enhancing operational efficiency. Nevertheless, challenges related to computational burden [40, 41], algorithm transparency, and real-time deployment remain. Addressing these limitations is essential to support the deployment of reliable and sustainable power systems.

The objective of the EVPSO approach is to minimize fuel consumption and pollutant emissions in thermal power plants while adhering to operational constraints such as inequality limits, ramp rate restrictions, and transmission losses. However, this objective introduces several challenges. The complexity of the optimization problem—due to multiple conflicting objectives—requires precise formulation to ensure the PSO algorithm performs effectively across system scales. Managing constraints through techniques like penalty functions adds to the computational overhead. Moreover, the algorithm’s robustness under uncertainties and dynamic load variations must be assured for practical utility. Finally, thorough validation through sensitivity analysis and large-scale simulations is necessary to confirm the consistency and reliability of EVPSO in real-world scenarios.

3.Methodology

The primary objective of multi-objective dispatch is to minimize energy generation costs while simultaneously satisfying fairness and inequality constraints.

3.1Objective function

This formulation meets the criteria for a dual-constraint optimization problem. Incorporating valve point loading (VPL) effects into the cost model makes it more realistic and advantageous, as it captures the nonlinearity and ripples in fuel cost characteristics. In this study, both the emission level and the cost function are represented using cubic equations to reflect their complex nature more accurately. The integrated economic and emission dispatch optimization problem is formulated accordingly. The fuel cost function F1i is defined in Equations 1 and 2 as follows:

$$F_{1i} = \sum_{i=1}^{m} f_{1i}(P_i) \quad (1)$$

Where F_{1i} is defines as shown in Equation 2.

$$F1i = \sum_{i=1}^{n} \Gamma_{1_i} + \Gamma_{2_i} P_i + \Gamma_{3_i} {P_i}^2 + abs\left(\Gamma_{4_i} sin\left\{\Gamma_{5_i}\left({P_i}^{min} - P_i\right)\right)\right\} + \frac{\Gamma_{6_i} {P_i}^3 Rs}{hr} \quad (2)$$

In Equation 2, the coefficients Γ_{1i}, Γ_{2i}, Γ_{3i}, Γ_{4i}, Γ_{5i} and Γ_{6i} represent the pricing parameters of the fuel cost function F_{1i} for thermal generating units. Among these, Γ_{4i} specifically accounts for the VPL effect, capturing the non-smooth ripples in the cost curve due to valve operation. P_i indicate the power output of unit i. These coefficients collectively define the fuel purchase cost structure used in modeling the thermal units' cost of fuel.

By quantifying the reduction in each type of emission, the specific environmental benefits achieved through the implementation of emission reduction strategies can be identified. This breakdown emphasizes the contributions made toward mitigating greenhouse gas emissions, such as carbon dioxide (CO_2), and reducing air pollutants like nitrous oxide (N_2O) and sulfur dioxide (SO_2), thereby demonstrating overall improvements in air quality and environmental sustainability. Presenting this detailed information enhances the transparency and clarity of the environmental impact assessment and strengthens the effectiveness of communication regarding the outcomes of emission reduction initiatives, as formulated in Equation 3.

$$F_{2_i} = \sum_{i=1}^{n} \Gamma_{7_i} + \Gamma_{8_i} P_i + \Gamma_{9_i} {P_i}^2 + abs(\eta_i exp(\delta_i P_i))\} + \Gamma_i {P_i}^3 T / hr \quad (3)$$

Where Γ_{7i}, Γ_{8i}, Γ_{9i}, η_i, δ_i and Γ_i represent the emission-related coefficients in the emission function F_{2i}, as defined in Equation 3. *Table 1*, *Table 2*, and *Table 3* present the values of the cost coefficients, emission coefficients, and the minimum and maximum power generation limits for the 15-unit, 40-unit, and 140-unit test systems, respectively. The values of Γ_{8i}, Γ_{9i}, η_i, δ_i and Γ_i are adopted in accordance with the IEEE standard test case system to ensure consistency and benchmarking validity.

Table 1 Cost and emission co-efficient with real power generation for 15 units

Unit	P_i^{min}	P_i	P_i^{max}	Γ_{1_i}	Γ_{2i}	Γ_{3i}	Γ_{4i}	Γ_{5i}	Γ_{6i}	Γ_{7i}	Γ_{8i}	Γ_{9i}	Γ_i	η_i	δ_i
450	45	450	405	0.009	0.828	130.5	-1224	0.135	0.013	0.013	0.04	54	-144	0.02	0.01
450	45	450	405	0.009	0.45	130.5	-1224	0.135	0.013	0.013	0.036	54	-144	0.02	0.01
125	12.5	125	112.5	0.002	0.125	36.25	-340	0.0375	0.003	0.003	0.01	15	-40	0.02	0.01
125	12.5	125	112.5	0.0025	0.125	36.25	-340	0.0375	0.0037	0.0037	0.01	15	-40	0.02	0.01
226	22.6	226	203.4	0.0045	0.226	65.54	-614.72	0.0678	0.0067	0.0067	0.0180	27.12	-72.32	0.02	0.01
455	45.5	455	409.5	0.0091	0.455	131.95	-1237.6	0.1365	0.0136	0.0136	0.0364	54.6	-145.6	0.02	0.01
460	46	460	414	0.0092	0.46	133.4	-1251.2	0.138	0.0138	0.0138	0.0368	55.2	-147.2	0.02	0.01
55	5.5	55	49.5	0.0011	0.055	15.95	-149.6	0.0165	0.0016	0.0016	0.0044	6.6	-17.6	0.02	0.01
20	2	20	18	0.0004	0.02	5.8	-54.4	0.006	0.0006	0.0006	0.0016	2.4	-6.4	0.02	0.01
30.5224	3.052	30.52	27.47	0.0006	0.0305	8.85	-83.01	0.009	0.009	0.009	0.0024	3.66	-9.767	0.02	0.01
69.2958	6.92	69.2	62.3	0.001	0.06	20.09	-188.48	0.02078	0.00207	0.00207	0.00554	8.31	-22.17	0.02	0.01
75	7.5	75	67.5	0.0015	0.075	21.75	-204	0.0225	0.00225	0.00225	0.006	9	-24	0.02	0.01
20	2	20	18	0.0004	0.02	5.8	-54.4	0.006	0.0006	0.0006	0.0016	2.4	-6.4	0.02	0.01
10	1	10	9	0.0002	0.01	2.9	-27.2	0.003	0.0003	0.0003	0.0008	1.2	-3.2	0.02	0.01
10	1	10	9	0.0002	0.01	2.9	-27.2	0.003	0.0003	0.0003	0.0008	1.2	-3.2	0.02	0.01

Table 2 Cost and emission co-efficient with real power generation for 40 units

Unit	P_i^{min}	P_i	P_i^{max}	Γ_{1_i}	Γ_{2i}	Γ_{3i}	Γ_{4i}	Γ_{5i}	Γ_{6i}	Γ_{7i}	Γ_{8i}	Γ_{9i}	Γ_i	η_i	δ_i
105.7	10.57	105.7	95.219	0.00211	0.105	30.68	-287.77	0.0317	0.00317	0.00317	0.008	12.6	-33.8	0.02	0.01
105.7	10.57	105.7	95.21	0.0021	0.10	30.68	-287.7	0.0317	0.00317	0.0031	0.0084	12.6	-33.85	0.02	0.01
92.39	9.239	92.39	83.159	0.0018	0.0923	26.795	-251.32	0.0277	0.0027	0.0027	0.0073	11.0	-29.56	0.02	0.01
174.7	17.47	174.7	157.25	0.003	0.174	50.67	-475.27	0.0524	0.00524	0.00524	0.0139	20.9	-55.91	0.02	0.01
82.7	8.27	82.7	74.51	0.0016	0.082	24.011	-225.21	0.0248	0.00248	0.00248	0.0066	9.93	-26.49	0.02	0.01
135	13.5	135	121.5	0.0027	0.135	39.15	-367.2	0.0405	0.00405	0.00405	0.0108	16.2	-43.2	0.02	0.01
254.5	25.45	254.5	229.13	0.0050	0.254	73.83	-692.51	0.0763	0.0076	0.00763	0.0203	30.5	-81.47	0.02	0.01
279.5	27.9	279.5	251.63	0.00559	0.2795	81.083	-760.511	0.083	0.0083	0.0083	0.0223	33.5	-89.47	0.02	0.01
279.5	27.95	279.5	251.63	0.0055	0.279	81.083	-760.511	0.083	0.0083	0.0083	0.0223	33.5	-89.47	0.02	0.01
125	12.5	125	112.5	0.0025	0.125	36.25	-340	0.0375	0.00375	0.00375	0.01	15	-40	0.02	0.01
89	8.9	89	80.1	0.00178	0.089	25.81	-242.08	0.0267	0.00267	0.00267	0.007	10.6	-28.48	0.02	0.01
89	8.9	89	80.1	0.00178	0.089	25.81	-242.08	0.0267	0.00267	0.00267	0.007	10.6	-28.48	0.02	0.01
209.7	20.97	209.7	188.78	0.0041	0.209	60.83	-570.54	0.0629	0.0062	0.0062	0.0167	25.1	-67.12	0.02	0.01
389.2	38.92	389.2	350.35	0.00778	0.3892	112.891	-1058.8	0.11678	0.0116	0.01167	0.031	46.7	-124.5	0.02	0.01
389.2	38.92	389.2	350.35	0.00778	0.3892	112.89	-1058.8	0.1167	0.0116	0.0116	0.0311	46.7	-124.5	0.02	0.01
389.2	38.92	389.2	350.35	0.00778	0.3892	112.891	-1058.	0.1167	0.01167	0.01167	0.0311	46.7	-124.5	0.02	0.01
484.2	48.72	484.2	435.55	0.00968	0.4842	140.44	-1317.2	0.1452	0.01452	0.01452	0.0387	58.1	-154.9	0.02	0.01
487.2	48.72	487.2	435.55	0.00974	0.4872	141.311	-1325.3	0.1461	0.01461	0.01461	0.0389	58.4	-155.9	0.02	0.01
506.2	50.62	506.2	455.65	0.01012	0.5062	146.82	-1377.0	0.1518	0.01518	0.01518	0.0405	60.7	-162.0	0.02	0.01
506.2	50.62	506.2	455.65	0.01012	0.5062	146.82	-1377.0	0.1518	0.01518	0.01518	0.0405	60.7	-162.0	0.02	0.01
518.2	51.82	518.2	466.45	0.01036	0.5182	150.30	-1409.7	0.1554	0.01554	0.01554	0.0414	62.1	-165.8	0.02	0.01
518.2	51.82	518.2	466.45	0.01036	0.5182	150.30	-1409.7	0.1554	0.01554	0.01554	0.0414	62.1	-165.8	0.02	0.01
518.2	51.82	518.2	466.45	0.01036	0.5182	150.30	-1409.7	0.1554	0.01554	0.01554	0.0414	62.1	-165.8	0.02	0.01
518.2	51.82	518.2	466.45	0.01036	0.518	150.30	-1409.7	0.1554	0.01554	0.01554	0.0414	62.1	-165.8	0.02	0.01
518.2	51.82	518.2	466.45	0.01036	0.5182	150.30	-1409.7	0.1554	0.01554	0.01554	0.0414	62.1	-165.8	0.02	0.01
518.2	51.82	518.2	466.45	0.01036	0.5182	150.30	-1409.7	0.1554	0.01554	0.01554	0.0414	62.1	-165.8	0.02	0.01
5	0.5	5	4.5	0.0001	0.005	1.45	-13.6	0.0015	0.00015	0.00015	0.0004	0.6	-1.6	0.02	0.01
5	0.5	5	4.5	0.0001	0.005	1.45	-13.6	0.0015	0.00015	0.00015	0.0004	0.6	-1.6	0.02	0.01
5	0.5	5	4.5	0.0001	0.005	1.45	-13.6	0.0015	0.00015	0.00015	0.0004	0.6	-1.6	0.02	0.01
82.79	8.279	82.79	74.519	0.00165	0.0827	24.0119	-225.21	0.0248	0.00248	0.00248	0.0066	9.93	-26.49	0.02	0.01
185	18.5	185	166.5	0.0037	0.185	53.65	-503.2	0.0555	0.00555	0.00555	0.0148	22.2	-59.2	0.02	0.01
185	18.5	185	166.5	0.0037	0.185	53.65	-503.2	0.0555	0.00555	0.00555	0.0148	22.2	-59.2	0.02	0.01
185	18.5	185	166.5	0.0037	0.185	53.65	-503.2	0.0555	0.00555	0.00555	0.0148	22.2	-59.2	0.02	0.01
159.7	15.97	159.7	143.81	0.00319	0.1597	46.341	-434.6	0.0479	0.00479	0.00479	0.0127	19.1	-51.13	0.02	0.01
189.3	18.93	189.3	170.45	0.00378	0.1893	54.925	-515.16	0.0568	0.00568	0.00568	0.0151	22.7	-60.60	0.02	0.01
195	19.5	195	175.5	0.0039	0.195	56.55	-530.4	0.0585	0.00585	0.00585	0.0156	23.4	-62.4	0.02	0.01
105	10.5	105	94.5	0.0021	0.105	30.45	-285.6	0.0315	0.00315	0.00315	0.0084	12.6	-33.6	0.02	0.01
105	10.5	105	94.5	0.0021	0.105	30.45	-285.6	0.0315	0.00315	0.00315	0.0084	12.6	-33.6	0.02	0.01
105	10.5	105	94.5	0.0021	0.105	30.45	-285.6	0.0315	0.00315	0.00315	0.0084	12.6	-33.6	0.02	0.01

Unit	P_i^{min}	P_i	P_i^{max}	Γ_{1_i}	Γ_{2i}	Γ_{3i}	Γ_{4i}	Γ_{5i}	Γ_{6i}	Γ_{7i}	Γ_{8i}	Γ_{9i}	Γ_i	η_i	δ_i
506.2	50.62	506.2	455.65	0.01012	0.5062	146.82	-1377.0	0.1518	0.0151	0.0151	0.0405	60.7	-162.0	0.02	0.01
105.7	10.57	105.7	95.219	0.00211	0.1057	30.681	-287.77	0.031	0.00317	0.00317	0.0084	12.6	-33.85	0.02	0.01

Table 3 Cost and emission co-efficient with real power generation for 140 units

Unit	P_i^{min}	P_i	P_i^{max}	Γ_{1_i}	Γ_{2i}	Γ_{3i}	Γ_{4i}	Γ_{5i}	Γ_{6i}	Γ_{7i}	Γ_{8i}	Γ_{9i}	Γ_i	η_i	δ_i
1	11.3	113.9	102.598	0.00227	0.113	33.05	-310.0	0.034	0.003	0.003	0.009	13.6	-36.47	0.02	0.01
2	15.9	159	143.1	0.00318	0.159	46.11	-432.4	0.047	0.0047	0.0047	0.012	19.0	-50.88	0.02	0.01
3	18.5	185	166.5	0.0037	0.185	53.65	-503.2	0.055	0.0055	0.0055	0.014	22.2	-59.2	0.02	0.01
4	18.5	185.99	167.4	0.00372	0.186	53.94	-505.9	0.055	0.0055	0.0055	0.014	22.3	-59.52	0.02	0.01
5	18.5	185	166.5	0.0037	0.185	53.65	-503.2	0.055	0.0055	0.0055	0.014	22.2	-59.2	0.02	0.01
6	18.4	184.99	166.493	0.003699	0.1849	53.647	-503.1	0.055	0.0055	0.0055	0.014	22.1	-59.19	0.02	0.01
7	48.5	485	436.5	0.0097	0.485	140.65	-1319.2	0.145	0.0145	0.0145	0.038	58.2	-155.2	0.02	0.01
8	48.4	484.99	436.49	0.0097	0.485	140.65	-1319.2	0.145	0.0145	0.0145	0.038	58.2	-155.2	0.02	0.01
9	49.1	491	441.9	0.00982	0.491	142.39	-1335.5	0.147	0.0147	0.0147	0.039	58.9	-157.1	0.02	0.01
10	49.1	491	441.9	0.00982	0.491	142.39	-1335.5	0.147	0.0147	0.0147	0.039	58.9	-157.1	0.02	0.01
11	49.1	491	441.9	0.00982	0.491	142.39	-1335.5	0.147	0.0147	0.0147	0.039	58.9	-157.1	0.02	0.01
12	49.1	491	441.9	0.00982	0.491	142.3	-1335.5	0.147	0.0147	0.0147	0.039	58.9	-157.1	0.02	0.01
13	50.1	501	450.9	0.01002	0.501	145.29	-1362.7	0.150	0.0150	0.0150	0.040	60.1	-160.3	0.02	0.01
14	50.3	503.9	453.599	0.01008	0.504	146.16	-1370.8	0.151	0.0151	0.0151	0.04	60.4	-161.2	0.02	0.01
15	50.1	501	450.9	0.01002	0.501	145.29	-1362.7	0.150	0.0150	0.0150	0.04	60.1	-160.3	0.02	0.01
16	49.9	499.99	450	0.01	0.5	145	-1360	0.15	0.015	0.015	0.04	60	-160	0.02	0.01
17	50	500	450	0.01	0.5	145	-1360	0.15	0.015	0.015	0.04	60	-160	0.02	0.01
18	49.9	499.99	449.99	0.01	0.5	145	-1360	0.15	0.015	0.015	0.04	60	-160	0.02	0.01
19	53.2	532	478.8	0.01064	0.532	154.28	-1447.0	0.159	0.0159	0.0159	0.04	63.8	-170.2	0.02	0.01
20	53.1	531.99	478.7999	0.01064	0.532	154.28	-1447.0	0.159	0.0159	0.0159	0.04	63.8	-170.2	0.02	0.01
21	54.4	544	489.6	0.01088	0.544	157.76	-1479.6	0.163	0.0163	0.0163	0.04	65.2	-174.0	0.02	0.01
22	54.4	544	489.6	0.01088	0.544	157.76	-1479.6	0.163	0.0163	0.0163	0.04	65.2	-174.0	0.02	0.01
23	49.5	495.99	446.4	0.00992	0.496	143.84	-1349.1	0.148	0.0148	0.0148	0.039	59.5	-158.7	0.02	0.01
24	49.4	494	444.6	0.00988	0.494	143.26	-1343.6	0.148	0.0148	0.0148	0.03	59.2	-158.0	0.02	0.01
25	50.1	501	450.9	0.01002	0.501	145.29	-1362.7	0.150	0.0150	0.0150	0.04	60.1	-160.3	0.02	0.01
26	50.1	501	450.9	0.01002	0.501	145.29	-1362.7	0.150	0.0150	0.0150	0.04	60.1	-160.3	0.02	0.01
27	50.1	501	450.9	0.01002	0.501	145.29	-1362.7	0.150	0.0150	0.0150	0.04	60.1	-160.3	0.02	0.01
28	50.1	501	450.9	0.01002	0.501	145.29	-1362.7	0.150	0.0150	0.0150	0.04	60.1	-160.3	0.02	0.01
29	49.5	495	445.5	0.0099	0.495	143.55	-1346.4	0.148	0.0148	0.0148	0.03	59.4	-158.4	0.02	0.01
30	50.1	501	450.9	0.01002	0.501	145.29	-1362.7	0.150	0.0150	0.0150	0.04	60.1	-160.3	0.02	0.01
31	49.5	495	445.5	0.0099	0.495	143.55	-1346.4	0.148	0.0148	0.0148	0.03	59.4	-158.4	0.02	0.01
32	23.9	239	215.1	0.00478	0.239	69.31	-650.08	0.071	0.0071	0.0071	0.01	28.6	-76.48	0.02	0.01
33	23.9	239	215.1	0.00478	0.239	69.31	-650.08	0.071	0.0071	0.0071	0.019	28.6	-76.48	0.02	0.01
34	76.8	768.99	692.0996	0.01538	0.769	223.01	-2091.6	0.230	0.0230	0.0230	0.06	92.2	-246.0	0.02	0.01
35	76.4	764	687.6	0.01528	0.764	221.56	-2078.0	0.229	0.0229	0.0229	0.061	91.6	-244.4	0.02	0.01
36	0.30	3.0004	2.70036	0.0000600	0.003	0.8701	-8.161	0.000	9E-05	9E-05	0.002	0.36	-0.960	0.02	0.01
37	0.3	3	2.7	0.00006	0.003	0.87	-8.16	0.000	0.0000	0.0000	0.002	0.36	-0.96	0.02	0.01
38	24.5	245	220.5	0.0049	0.245	71.05	-666.4	0.073	0.0073	0.0073	0.019	29.4	-78.4	0.02	0.01
39	24.4	244.99	220.498	0.00489	0.244	71.04	-666.39	0.073	0.007	0.0073	0.019	29.3	-78.39	0.02	0.01
40	24.5	245.99	221.397	0.00491	0.2459	71.33	-669.1	0.073	0.0073	0.0073	0.019	29.5	-78.7	0.02	0.01
41	24.5	245.99	221.3967	0.004919	0.245	71.33	-669.11	0.073	0.007	0.0073	0.019	29.5	-78.71	0.02	0.01
42	24.5	245.99	221.399	0.0049	0.246	71.34	-669.12	0.073	0.0073	0.0073	0.019	29.5	-78.72	0.02	0.01
43	24.5	245	220.5	0.0049	0.245	71.05	-666.4	0.073	0.0073	0.0073	0.019	29.4	-78.4	0.02	0.01
44	24.4	244.99	220.199	0.00489	0.2449	71.049	-666.39	0.073	0.0073	0.0073	0.019	29.3	-78.3	0.02	0.01
45	24.4	245.99	221.5372	0.00491	0.2459	71.339	-669.11	0.073	0.0073	0.0073	0.019	29.5	-78.7	0.02	0.01
46	24.5	245.99	221.399	0.00492	0.246	71.34	-669.12	0.073	0.0073	0.0073	0.019	29.5	-78.72	0.02	0.01
47	24.5	245	220.5	0.0049	0.245	71.05	-666.4	0.073	0.0073	0.0073	0.019	29.4	-78.4	0.02	0.01
48	24.5	245	220.5	0.0049	0.245	71.05	-666.4	0.073	0.0073	0.0073	0.019	29.4	-78.4	0.02	0.01
49	24.5	245	220.5	0.0049	0.245	71.05	-666.4	0.073	0.0073	0.0073	0.019	29.4	-78.4	0.02	0.01
50	16	160	144	0.0032	0.16	46.4	-435.2	0.048	0.0048	0.0048	0.012	19.2	-51.2	0.02	0.01
51	16.0	160.00	144.0085	0.0032002	0.1600	46.402	-435.22	0.048	0.0048	0.0048	0.012	19.2	-51.20	0.02	0.01
52	16	160	144	0.0032	0.16	46.4	-435.2	0.048	0.0048	0.0048	0.012	19.2	-51.2	0.02	0.01
53	16.0	160.00	144.008	0.0032002	0.1600	46.402	-435.22	0.048	0.0048	0.0048	0.012	19.2	-51.20	0.02	0.01
54	17.5	175	157.5	0.0035	0.175	50.75	-476	0.052	0.0052	0.0052	0.014	21	-56	0.02	0.01
55	17.5	175	157.5	0.0035	0.175	50.75	-476	0.052	0.0052	0.0052	0.014	21	-56	0.02	0.01
56	9.80	98.000	88.200	0.0019600	0.0980	28.420	-266.56	0.029	0.0029	0.0029	0.007	11.7	-31.36	0.02	0.01
57	19.3	193	173.7	0.00386	0.193	55.97	-524.96	0.057	0.0057	0.0057	0.015	23.1	-61.76	0.02	0.01
58	29.6	296.99	267.299	0.0059399	0.2969	86.129	-807.83	0.089	0.0089	0.0089	0.023	35.6	-95.03	0.02	0.01
59	30.3	303.19	272.876	0.006063	0.3031	87.927	-824.69	0.090	0.0090	0.0090	0.024	36.3	-97.02	0.02	0.01
60	15.8	158	142.2	0.00316	0.158	45.82	-429.76	0.047	0.0047	0.0047	0.012	18.9	-50.56	0.02	0.01
61	9.3	93.000	83.70009	0.0018600	0.093	26.970	-252.96	0.027	0.0027	0.0027	0.007	11.1	-29.76	0.02	0.01
62	50.5	505.99	455.3993	0.0101199	0.5059	146.73	-1376.3	0.151	0.0151	0.0151	0.04	60.7	-161.9	0.02	0.01
63	50.6	506	455.4	0.01012	0.506	146.74	-1376.3	0.151	0.0151	0.0151	0.04	60.7	-161.9	0.02	0.01
64	48.4	484.99	436.498	0.00969	0.4849	140.64	-1319.1	0.145	0.014	0.0145	0.038	58.1	-155.1	0.02	0.01
65	25.2	252.06	226.8621	0.005041	0.252	73.100	-685.6	0.075	0.0075	0.0075	0.02	30.2	-80.6	0.02	0.01
66	48.5	485	436.5	0.0097	0.485	140.65	-1319.2	0.145	0.0145	0.0145	0.03	58.2	-155.2	0.02	0.01
67	48.4	484.99	436.5087	0.0096999	0.4849	140.64	-1319.2	0.145	0.0145	0.0145	0.03	58.1	-155.2	0.02	0.01
68	12.5	125	112.5	0.0025	0.125	36.25	-340	0.037	0.0037	0.0037	0.01	15	-40	0.02	0.01
69	28.9	289.78	260.8039	0.0057956	0.2897	84.036	-788.20	0.086	0.0086	0.0086	0.023	34.7	-92.73	0.02	0.01
70	13.9	139.16	125.249	0.00278	0.1391	40.358	-378.53	0.041	0.0041	0.0041	0.011	16.6	-44.53	0.02	0.01
71	36.1	361.93	325.738	0.007238	0.361	104.96	-984.4	0.108	0.0108	0.010	0.0289	43.4	-115.8	0.02	0.01
72	19.1	191.02	171.926	0.00382	0.191	55.398	-519.59	0.057	0.0057	0.0057	0.0152	22.9	-61.12	0.02	0.01
73	25.7	257.13	231.424	0.005142	0.257	74.570	-699.4	0.077	0.0077	0.0077	0.0205	30.8	-82.28	0.02	0.01
74	17.1	171.68	154.51	0.003433	0.1716	49.78	-466.9	0.051	0.0051	0.005	0.013	20.6	-54.93	0.02	0.01
75	25.2	252.06	226.8621	0.0050413	0.2520	73.100	-685.62	0.075	0.0075	0.0075	0.0201	30.2	-80.66	0.02	0.01
76	48.5	485	436.5	0.0097	0.485	140.65	-1319.2	0.145	0.0145	0.0145	0.0388	58.2	-155.2	0.02	0.01
77	48.4	484.99	436.498	0.009699	0.4849	140.64	-1319.2	0.145	0.0145	0.014	0.0388	58.1	-155.2	0.02	0.01

Unit	P_i^{min}	P_i	P_i^{max}	Γ_{1_i}	Γ_{2i}	Γ_{3i}	Γ_{4i}	Γ_{5i}	Γ_{6i}	Γ_{7i}	Γ_{8i}	Γ_{9i}	Γ_i	η_i	δ_i
78	12.5	125	112.5	0.0025	0.125	36.25	-340	0.037	0.0037	0.0037	0.01	15	-40	0.02	0.01
79	28.9	289.78	260.8039	0.0057956	0.2897	84.036	-788.20	0.086	0.0086	0.0086	0.0231	34.7	-92.73	0.02	0.01
80	13.9	139.16	125.2490	0.0027833	0.1391	40.358	-378.5	0.041	0.0041	0.0041	0.0111	16.6	-44.53	0.02	0.01
81	36.1	361.93	325.7384	0.0072386	0.3619	104.96	-984.45	0.108	0.0108	0.0108	0.0289	43.4	-115.8	0.02	0.01
82	19.1	191.02	171.9264	0.0038205	0.1910	55.398	-519.59	0.057	0.0057	0.0057	0.0152	22.9	-61.12	0.02	0.01
83	25.7	257.13	231.4248	0.0051427	0.2571	74.570	-699.41	0.077	0.0077	0.0077	0.0205	30.8	-82.28	0.02	0.01
84	17.1	171.68	154.513	0.0034	0.1716	49.787	-466.9	0.051	0.005	0.005	0.0137	20.6	-54.9	0.02	0.01
85	25.2	252.71	227.4422	0.0050542	0.2527	73.287	-687.38	0.075	0.0075	0.0075	0.0202	30.3	-80.86	0.02	0.01
86	48.5	485	436.5	0.0097	0.485	140.65	-1319.2	0.145	0.0145	0.0145	0.0388	58.2	-155.2	0.02	0.01
87	48.4	484.99	436.498	0.00969	0.484	140.6	-1319.2	0.145	0.0145	0.0145	0.0388	58.1	-155.2	0.02	0.01
88	12.5	125	112.5	0.0025	0.125	36.25	-340	0.037	0.0037	0.0037	0.01	15	-40	0.02	0.01
89	28.9	289.78	260.8039	0.0057956	0.2897	84.036	-788.20	0.086	0.0086	0.0086	0.0231	34.7	-92.7	0.02	0.01
90	13.7	137.16	123.4490	0.0027433	0.137	39.778	-373.09	0.041	0.004	0.0041	0.0109	16.4	-43.89	0.02	0.01
91	36.1	361.93	325.7420	0.0072387	0.3619	104.96	-984.46	0.108	0.0108	0.0108	0.0289	43.4	-115.8	0.02	0.01
92	19.1	191.02	171.9264	0.003820	0.1910	55.398	-519.5	0.057	0.0057	0.0057	0.0152	22.9	-61.1	0.02	0.01
93	25.7	257.13	231.424	0.005142	0.2571	74.570	-699.41	0.077	0.0077	0.0077	0.0205	30.8	-82.28	0.02	0.01
94	17.1	171.68	154.513	0.0034336	0.1716	49.78	-466.9	0.051	0.005	0.005	0.0137	20.6	-54.93	0.02	0.01
95	25.2	252.7	227.442	0.0050542	0.2527	73.28	-687.3	0.07	0.0075	0.0075	0.0202	30.3	-80.86	0.02	0.01
96	39.4	394.67	357.204	0.00789	0.394	114.4	-1073.5	0.118	0.011	0.011	0.0315	47.3	-126.2	0.02	0.01
97	32.5	325.00	292.5042	0.0065001	0.3250	94.251	-884.01	0.097	0.0097	0.0097	0.026	39.0	-104.0	0.02	0.01
98	52.8	528	475.2	0.01056	0.528	153.12	-1436.1	0.158	0.0158	0.0158	0.0422	63.3	-168.9	0.02	0.01
99	52.8	528	475.2	0.01056	0.528	153.12	-1436.1	0.158	0.0158	0.0158	0.0422	63.3	-168.9	0.02	0.01
100	53.6	536.9	483.299	0.01074	0.537	155.73	-1460.6	0.161	0.0161	0.0161	0.0429	64.4	-171.8	0.02	0.01
101	5.1	51	45.9	0.00102	0.051	14.79	-138.72	0.015	0.0015	0.0015	0.0040	6.12	-16.32	0.02	0.01
102	11	110	99	0.0022	0.11	31.9	-299.2	0.033	0.0033	0.0033	0.0088	13.2	-35.2	0.02	0.01
103	11	110	99	0.0022	0.11	31.9	-299.2	0.033	0.0033	0.0033	0.0088	13.2	-35.2	0.02	0.01
104	11	110	99	0.0022	0.11	31.9	-299.2	0.033	0.0033	0.0033	0.0088	13.2	-35.2	0.02	0.01
105	20.2	202.00	181.8000	0.00404	0.202	58.58	-549.44	0.060	0.0060	0.0060	0.0161	24.2	-64.64	0.02	0.01
106	20.2	202.00	181.8000	0.00404	0.202	58.58	-549.44	0.060	0.0060	0.0060	0.0161	24.2	-64.64	0.02	0.01
107	17.0	170.00	153.0002	0.0034	0.17	49.3	-462.4	0.051	0.0051	0.0051	0.0136	20.4	-54.4	0.02	0.01
108	17.0	170.00	153.0013	0.0034000	0.1700	49.300	-462.40	0.051	0.0051	0.0051	0.0136	20.4	-54.40	0.02	0.01
109	17.5	175.51	157.960	0.00351	0.1755	50.898	-477.39	0.052	0.0052	0.0052	0.0140	21.0	-56.16	0.02	0.01
110	17	170	153	0.0034	0.17	49.3	-462.4	0.051	0.0051	0.0051	0.0136	20.4	-54.4	0.02	0.01
111	57.0	570.4	513.36	0.011408	0.5704	165.41	-1551.4	0.171	0.0171	0.0171	0.0456	68.4	-182.5	0.02	0.01
112	54.2	542.5	488.25	0.01085	0.5425	157.32	-1475.6	0.162	0.0162	0.0162	0.0434	65.1	-173.6	0.02	0.01
113	83.2	832.8	749.52	0.016656	0.8328	241.51	-2265.2	0.249	0.0249	0.0249	0.0666	99.9	-266.4	0.02	0.01
114	83.2	832.5	749.25	0.01665	0.8325	241.42	-2264.4	0.249	0.0249	0.0249	0.0666	99.9	-266.4	0.02	0.01
115	67.7	677	609.3	0.01354	0.677	196.33	-1841.4	0.203	0.0203	0.0203	0.0541	81.2	-216.6	0.02	0.01
116	71.4	714	642.6	0.01428	0.714	207.06	-1942.0	0.214	0.0214	0.0214	0.0571	85.6	-228.4	0.02	0.01
117	71.4	714	642.6	0.01428	0.714	207.06	-1942.0	0.214	0.0214	0.0214	0.0571	85.6	-228.4	0.02	0.01
118	71.4	714.99	643.5099	0.0143	0.715	207.35	-1944.8	0.214	0.0214	0.0214	0.0572	85.8	-228.8	0.02	0.01
119	95.8	958.99	863.1099	0.01918	0.959	278.11	-2608.4	0.287	0.0287	0.0287	0.0767	115.	-306.8	0.02	0.01
120	95.3	953	857.7	0.01906	0.953	276.37	-2592.1	0.285	0.0285	0.0285	0.0762	114.	-304.9	0.02	0.01
121	94.2	942.9	848.61	0.018858	0.9429	273.44	-2564.6	0.282	0.0282	0.0282	0.0754	113.	-301.7	0.02	0.01
122	92.9	929	836.1	0.01858	0.929	269.41	-2526.8	0.278	0.0278	0.0278	0.0743	111.	-297.2	0.02	0.01
123	93	930	837	0.0186	0.93	269.7	-2529.6	0.279	0.0279	0.0279	0.0744	111.	-97.6	0.02	0.01
124	87.1	871	783.9	0.01742	0.871	252.59	-2369.1	0.261	0.0261	0.0261	0.0696	104.	-278.7	0.02	0.01
125	87.5	875.9	788.31	0.017518	0.8759	254.01	-2382.4	0.262	0.0262	0.0262	0.0700	105.	-280.2	0.02	0.01
126	86.8	868.7	781.83	0.017374	0.8687	251.92	-2362.8	0.26	0.0260	0.0260	0.0694	104.	-277.9	0.02	0.01
127	87.2	872.4	785.16	0.017448	0.8724	252.99	-2372.9	0.261	0.0261	0.0261	0.0697	104.	-279.1	0.02	0.01
128	86.6	866.7	780.03	0.017334	0.8667	251.34	-2357.4	0.260	0.0260	0.0260	0.0693	104.	-277.3	0.02	0.01
129	85.9	859.79	773.8199	0.017196	0.8598	249.34	-2338.6	0.257	0.0257	0.0257	0.0687	103.	-275.1	0.02	0.01
130	87.7	877.9	790.11	0.017558	0.8779	254.59	-2387.8	0.263	0.0263	0.0263	0.0702	105.	-20.9	0.02	0.01
131	86.8	868.7	781.83	0.017374	0.8687	251.92	-2362.8	0.260	0.0260	0.0260	0.0694	104.	-277.9	0.02	0.01
132	87.2	872.4	785.16	0.017448	0.8724	252.99	-2372.9	0.261	0.0261	0.0261	0.0697	104.	-279.1	0.02	0.01
133	86.6	866.7	780.03	0.017334	0.8667	251.34	-2357.4	0.260	0.026	0.0260	0.0693	104.	-277.3	0.02	0.01
134	85.9	859.79	773.8199	0.01719	0.859	249.34	-2338.6	0.257	0.0257	0.0257	0.068	103.	-275.1	0.02	0.01
135	87.7	877	0.177	0.01754	0.877	254.33	-2385.4	0.263	0.0263	0.0263	0.0701	105.	-280.6	0.02	0.01
136	8.90	89.001	80.1009	0.00178	0.0890	25.810	-242.08	0.026	0.0026	0.0026	0.0071	10.6	-28.48	0.02	0.01
137	8.9	89	80.1	0.00178	0.089	25.81	-242.08	0.02	0.002	0.0026	0.007	10.6	-28.48	0.02	0.01
138	8.9	89	80.1	0.00178	0.089	25.81	-242.08	0.026	0.0026	0.0026	0.0071	10.6	-28.48	0.02	0.01
139	23.9	239.00	215.100	0.00478	0.239	69.31	-650.08	0.071	0.0071	0.0071	0.0191	28.6	-76.48	0.02	0.01
140	23.9	239.00	215.1008	0.0047800	0.2390	69.310	-650.08	0.071	0.0071	0.0071	0.0191	28.6	-76.48	0.02	0.01

3.2Equality constraint

This group of limits also includes balancing power levels or consumption limitations [9]. This limitation specifies that the entire system's production ($\sum_{i=1}^{m} P_i$) as shown in Equation 4 must remain in balance with the overall total system loads. In other words, it can be expressed as overall losses (P_D), emphasizing the system losses (P_L), and is alternatively represented by Equation 4.

$$\sum_{i=1}^{m} P_i - P_D - P_L \quad (4)$$

Where P_L, as shown in Equation 5, is determined by multiplying the power outputs of the generating units with the corresponding loss coefficients, as defined by the following expression.

$$P_L = \sum_{i=1}^{m} \sum_{j=1}^{m} P_i B_{ij} P_j + \sum_{i=1}^{m} B_{oi} P_i + B_{00} \quad (5)$$

By analyzing how transmission losses influence the performance of the optimization algorithm, one can assess the trade-offs between minimizing losses and achieving the desired objectives, such as cost reduction or emission mitigation. Understanding the impact of transmission losses on the efficiency and cost-effectiveness of the vector PSO method can provide valuable insights into the practical feasibility and effectiveness of the approach in real-world power system applications.

3.3Inequality limitation

Limitation of generation capacity:

There must be a permissible range between the upper and lower generation limits, as defined by Equation 6.

$$P_i^{min} \leq P_i \leq P_i^{max} \quad (6)$$

where i=1,2,...m

Ramp rate limitations

Ramp rate constraints limit how quickly generators can change their output over time, thereby preventing abrupt power fluctuations that could destabilize the power system. For each generator, the actual power output must remain within the allowable range defined by its upper and lower ramp rate bounds, as described in [10–12]. To ensure that solutions generated by the vector PSO optimization model for ELD comply with these ramp rate and system loss constraints, both the objective function and the particle velocity update equation are appropriately modified [42, 43].

Ramp rate constraints are enforced by adjusting the particle velocity update equation in the vector theta PSO model [44], thereby limiting the change in generator output between successive iterations. This ensures that generator output transitions smoothly and remains within acceptable ramping limits.

Additionally, penalty terms can be introduced into the objective function to discourage violations of ramp rate constraints. These penalties increase the objective function value when the ramp rate is exceeded, guiding the algorithm to favor feasible solutions that respect the imposed limitations.

$$max\left(P_i^{min}, P_i^{0} - DR_i\right) \leq P_i \leq min\left(P_i^{max}, P_i^{0} + UR_i\right) \quad (7)$$

System losses

System losses refer to the power dissipated as heat in transmission lines and other components, representing inefficiencies in power delivery. Reducing these losses is crucial for enhancing the overall efficiency of the power system in ELD applications.

To incorporate system losses into the optimization model, an additional term representing total transmission losses is included in the objective function. This term is typically proportional to the sum of the squares of power flows, accurately capturing the loss behavior in the system.

By including this term, the vector PSO algorithm not only minimizes the generation cost but also considers the impact of losses. The optimization process thus aims to balance economic efficiency with transmission reliability and energy conservation.

Implementation

To incorporate both generation cost and system losses into the optimization model, these components are combined within the objective function, with appropriate weighting factors to reflect the relative importance of each objective. To ensure that the algorithm satisfies ramp rate constraints, the particle velocity update equation is modified to limit variations in generator output between successive iterations. This modification helps maintain compliance with ramp rate limitations and promotes smoother transitions in power output. The effectiveness of the modified vector theta PSO optimization model should be validated through a series of experiments. These evaluations aim to assess the algorithm’s capability to generate feasible solutions that minimize generation costs, reduce system losses, and comply with ramp rate constraints. By integrating ramp rate and system loss constraints, the vector PSO model becomes more robust and efficient for solving ELD problems, while also enhancing the stability and operational reliability of the power system. Accordingly, the generator constraints initially defined in Equation 6 are adjusted to incorporate these considerations, as represented in the modified form shown in Equation 7.

3.4Role and function of vector θ –PSO optimization technique

This work presents a vector PSO technique inspired by electromagnetic principles to reduce fuel consumption and pollutant emissions in thermal power generation. The generating units are assumed to be thermally and permanently online to ensure the consistent performance of the proposed model, which addresses multiple constraints including equality and inequality limits, ramp rate restrictions, VPL effects, and transmission losses [13–15]. To optimize the cubic fuel cost and emission functions for 15-unit, 40-unit, and 140-unit systems, an electromagnetic-based vector optimization approach is employed, incorporating system losses and other critical operational parameters. The displacement vector used in this study, as illustrated in *Figure 1*, assumes that all alternators are spatially distributed in a circular coordinate system. This configuration proves effective in determining the angular component of complex power generation.

To evaluate the long-term reliability and stability of the proposed method, it is necessary to analyze its performance under extended time horizons and varying operational conditions. This includes assessing the algorithm's robustness in managing system uncertainties, dynamic load changes, and fluctuations in system parameters. Additionally, comprehensive sensitivity analyses and performance evaluations are essential to gauge the consistency and effectiveness of the vector PSO approach in solving multi-objective ELD problems. Monitoring its behavior across different operating scenarios provides valuable insights into the method's practical applicability and informs decisions regarding its suitability and reliability for real-world power system operations.

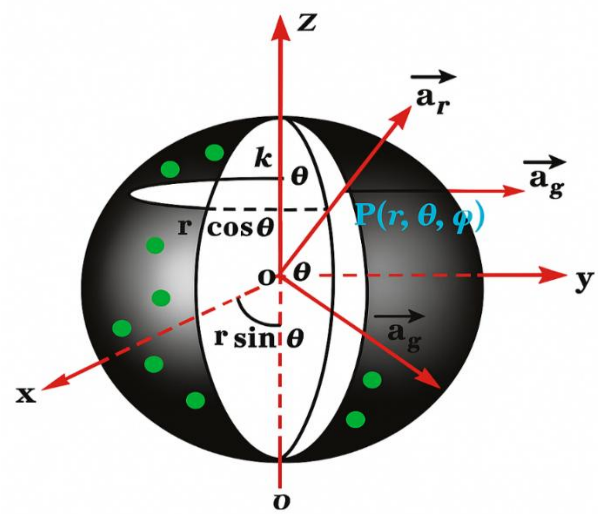

Figure 1 Spatial allocation of alternators for the 15-unit system

The elementary displacement vector in spherical coordinate system is given by Equation 8;

$$\vec{dl} = dr\vec{ar} + rd\theta\vec{a\theta} + r sin\theta d\phi \vec{a\phi} \qquad (8)$$

Where, $d\vec{l}$ is the displacement vector in spherical coordinate system shown in Equation 8 &r, θ & ϕ are the action parameters of spherical coordinate system.

$$\overrightarrow{dl} = rd\theta\overrightarrow{d\theta}$$

$$\theta_{pi} = \int \frac{d\vec{l}}{r}$$

θ_{pi} in spherical coordinate system is expressed in Equation 9 as under;

$$\Rightarrow \theta_{pi} = \int \frac{d\vec{r}}{r}\overrightarrow{ar} + \int \frac{rd\theta}{r}\overrightarrow{a\theta} + \int \frac{rsin\theta d\phi}{r}\overrightarrow{a\phi} \quad (9)$$

$\theta_{p1i} = -75^0$
$\theta_{p2i} = 75^0$
$\theta = 90^0$
$\phi_{p1} = -45^0$

$\phi_{p2} = 45^0$, r =1pu

Using the above values in Equation 9, $\theta_{pi}$is expressed in Equation 10 as under;

$$\theta_{\text{pi}} = \ln r\, \vec{a}r + (\theta_{p2i} - \theta_{p1i})a\vec{\theta} + sin\theta_{pi}(\phi_{p2} - \phi_{p1})a\overrightarrow{\phi} \qquad (10)$$

$$\Rightarrow \theta_{\text{pi}} = (\theta_{p2i} - \theta_{p1i})a\vec{\theta} + sin\theta_{pi}(\phi_{p2} - \phi_{p1})a\vec{\phi}$$
$$\Rightarrow \theta_{\text{pi}} = 90 \times [\sqrt{(1.66)^2 + (1)^2}]$$
$$\Rightarrow \theta_{\text{pi}} = 174.4^0$$

To adjust the geographic distance of the i^{th} component from the load center of the power plant, a position vector is utilized. The general procedure for generating a new position vector—comprising the phase angle, maximum particle velocity, and the velocity update term V_{idn}—is outlined in step 5 of the vector PSO algorithm. The calculation of V_{idn} requires several parameters from the vector PSO framework, including the acceleration coefficients c_1 and c_2, random numbers r_1 and r_2, and the inertia weight w, all of which must be appropriately estimated. Once the new position vector is determined, the corresponding production cost and emission level are updated accordingly, and the results are used for comparative performance analysis.

3.5Constraint handling technique for handling accuracy and effectiveness of the PSO algorithm

Solving the ELD problem becomes challenging in the presence of multiple constraints. Over the past two decades, numerous methods have been proposed to address constrained optimization problems, with constraint-handling techniques remaining a key area of focus. Among these, the penalty function method is one of the most widely adopted approaches. The core idea behind this method is to transform a constrained optimization problem into an unconstrained one by adding a penalty term to the objective function value, which reflects the degree of constraint violation in a given solution. This approach is favored for its simplicity and effectiveness. Accordingly, the penalty function technique is employed in this study. Specifically, a variant of the Lagrangian relaxation-based penalty method is used to convert the constrained ELD problem into an unconstrained optimization problem, as expressed in Equation 11.

$$F(x) = f(x) + w1 \times (sum\_viol) + w2 \times num\_viol \quad (11)$$

Where f(x) is the objective function of problem, $w1$ and $w2$ are penalty factors, *sum_viol* denotes the sum of all the amounts by which the constraints are violated, and *num_viol* denotes the number of constraints violation.

In the proposed vector PSO technique, four benchmark functions are employed to demonstrate the effectiveness of the improved algorithm. These functions include Rosenbrock, Rastrigin, Schwefel, and Ackley, each of which is commonly used in global optimization studies to evaluate the performance of metaheuristic algorithms. The objective is to assess the algorithm's ability to converge toward the global minimum, typically set to zero for these functions. The operational bounds and optimal values for each of these benchmark functions are defined and evaluated as presented in Equations 12 to 15.

$$f(x) = \sum_{i=1}^{n-1}(100(x_{i+1} - x^2{}_i)^2 + (x_i - 1)^2), Range(0.002 - 135), Optimal\ value\ is\ 0 \quad (12)$$

$$f(x) = \sum_{i=1}^{n-1}(x_i{}^2 - 10cos(2\Pi x_i) + 10), Range(0.0001 - 151), Optimal\ valueis\ 0 \quad (13)$$

$$f_6(x) = 418.98n - \sum_{i=1}^{n}(x_i{}^2\, sin(\sqrt{|x_i|}), Range(0.00006 - 279), Optimal\ value\ is\ 0 \quad (14)$$

$$f(x) = -20exp(-0.2\sqrt{\frac{1}{n}}\sum_{i=1}^{n} cos(2\Pi x_i) + 20 + e, Range(0.002 - 150), Optimal\ value\ is\ 0 \quad (15)$$

3.6Formulation of Electromagnetic based Vector PSO Algorithm

Step-1: Utilize a method of creating θ_{pi} electromagnetic gradients.

Step-2: Every Nth random particle, individually, $x_{gi} = |x_{gi}| < \theta_{pi}$ (i=1 to N) are generated with a D dimensional vector $|X_{gi}|$ and a corresponding scalar phase angle θ_{pi} & likewise limited by initial speed $Vid_{max(i)}$are organized as follows for individual particles;

$x_{gi}=x_{min,d}+r1(x_{max}-x_{min})$

$Vid_{max(i)} \rightarrow (0to2\pi)$

Step-3: The positions and velocities of each one throughout each iteration are determined using the equations underneath.

$V_{id_{max,i}} = x_{gi}, i = 1 ...$

$x_{gi} = x_{gi} + V_{id}$

Step 4: The P_{best} i.e., P_{Thpi} and G_{best} i.e. G_{Thpi} , the calculation of positions are as follows,

$P_{best\,\theta pi} = cos\theta_{pi}{}^{2sin\theta_{pi}}$

$G_{best\,\theta pi} = sin\theta_{pi}{}^{2cos\theta_{pi}}$

Step 5: The computed phase angle and greatest particle velocities are presented below.

$$f(\theta_{pi}) = v_{id} = \frac{X_{max} - X_{min}}{2} sin\theta_{id} + \frac{X_{max} + X_{min}}{2}$$

$Where, d = 1,2 \ldots D\ \&\ i = 1,2 \ldots S$

$\theta_{pin} = \theta_{pi} + |cos\theta_{i_d} + sin\theta_{i_d}|x2\pi$

$V_{idn} = wx_{gi} + c_1r_1(P_{best\,\theta pi} - x_{gi}) + c_2r_2(G_{best\,\theta pi} - x_{gi})$

The update positions are determined as under;

$x_{gin} = x_{gi} + v_{idn}, Where\ x_{gi} = ComplexPower$

$x_{gin} = P_{in}$

Step 6: Steps 4 and 5, which were selected from a list of functions included in Equations 11 to 15, and Provided the empirical formula as under.

Step 7: The target functions and emission functionality with and without loss are computed using the values obtained in stages 5 and 6 [17–19]. The Flow chart for electromagnetic based vector PSO employing steps 1 to 7 above is described in *Figure 2* as under.

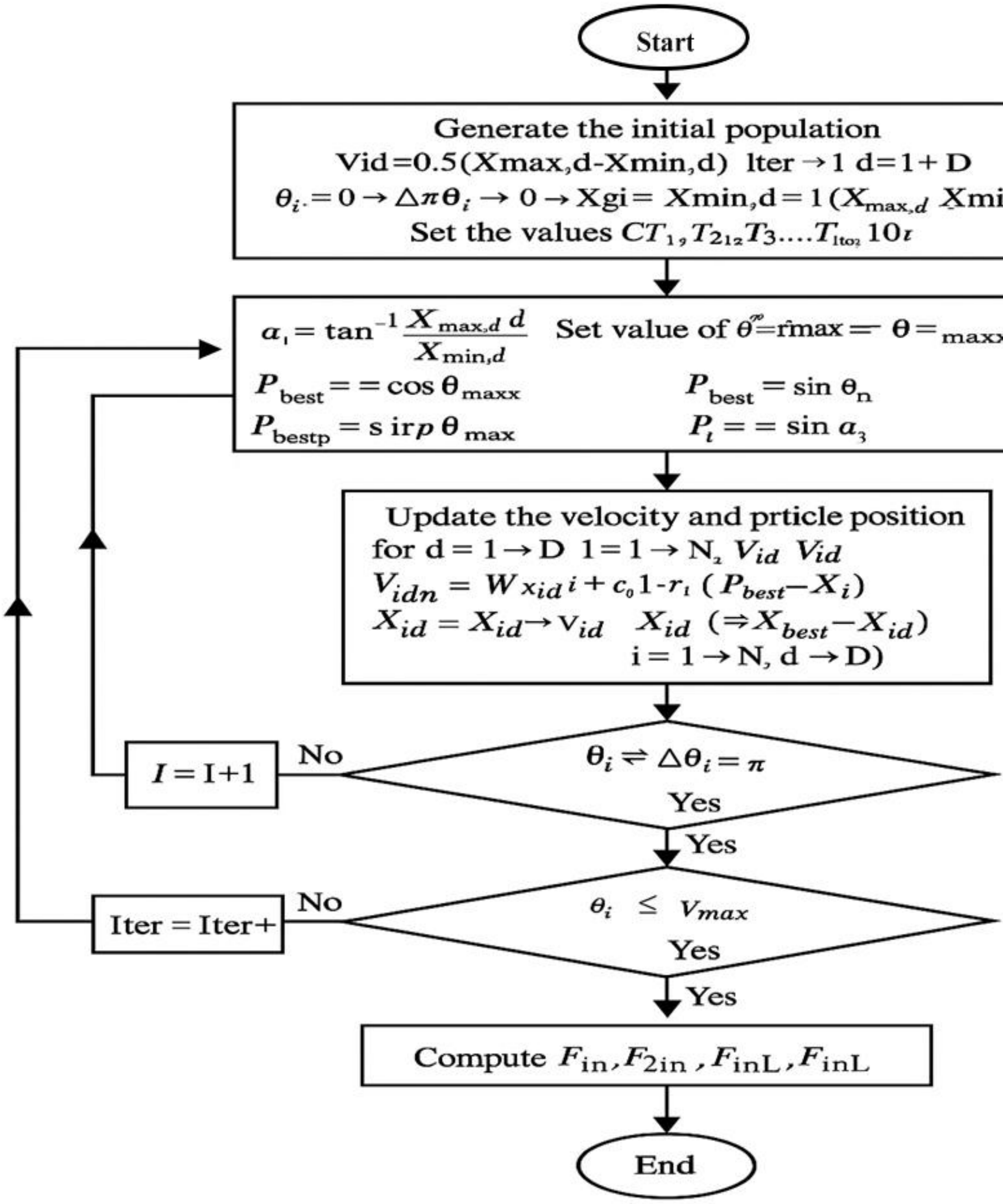

Figure 2 Flowchart of electromagnetic-based vector θ-PSO

4.Results and discussion

MATLAB has been used for the implementation. The system description for testing is provided below.

System description for testing

Integrating renewable energy sources, such as solar and wind power, into the ELD process presents significant challenges due to their intermittent and variable nature [45, 46]. To address these challenges, the vector PSO method [47], known for its effectiveness in optimizing complex systems, has been incorporated into the ELD framework. This integration aims to enhance the overall efficiency and effectiveness of ELD operations [48].

By leveraging the optimization capabilities of vector PSO, it is possible to improve the scheduling and utilization of renewable energy sources alongside conventional generation units. This approach facilitates cost savings, improves system reliability, and reduces environmental impact. Consequently, it presents a promising strategy for addressing the integration challenges of renewable energy sources while maintaining economic viability.

The cost savings achieved using the vector PSO [49, 50] approach in a 15-unit power system are presented in *Table 4.* Additionally, fuel cost (in Rs./hr) and emission levels (in tons/hr) for systems with 15, 40, and 140 units optimized using the Weight Improved Particle Swarm Optimization (WIPSO) [51], Bacterial Foraging Optimization (BFO) [52], and Gray Wolf Optimization (GWO) [53] methods—both with and without considering transmission losses—are detailed in *Tables 5, 6*, and *7*, respectively.

Table 4 Fuel cost (Rs./hr) and emission (tons/hr) for 15-Unit, 40-Unit, and 140-Unit Vector θ–PSO Systems with and without transmission loss

Power demand in (MW)	**Fuel price in rupees per hour and emission in tonnes per hour for 15-unit vector θ –PSO system without and with transmission loss**	**Fuel price in rupees per hour and emission in tonnes per hour for 40-unit vector θ –PSO system without and with transmission loss**	**Fuel price in rupees per hour and emission in tonnes per hour for 140-unit vector θ –PSO system without and with transmission loss**
2580/10303/55984	3310000	200×10^{6}	125×10^{7}
2580/10303/55984	5100000	5800000	0.4×10^{9}
2580/10303/55984	2205000	325×10^{7}	4×10^{9}
2580/10303/55984	3650000	4×10^{6}	0.2×10^{9}

Table 5 Fuel cost (Rs./hr) and emission (tons/hr) for 15-Unit, 40-Unit, and 140-Unit WIPSO systems with and without transmission loss

Power demand in (MW)	**Fuel price in rupees per hour and emission in tonnes per hour for 15-unit WIPSO system without and with transmission loss**	**Fuel price in rupees per hour and emission in tonnes per hour for 40-unit WIPSO system without and with transmission loss**	**Fuel price in rupees per hour and emission in tonnes per hour for 140-unit WIPSO system without and with transmission loss**
2580/10303/55984	3310001	202×10^{6}	126×10^{7}
2580/10303/55984	5100002	5800003	0.5×10^{9}
2580/10303/55984	2205003	326.6×10^{7}	5×10^{9}
2580/10303/55984	3650004	5×10^{6}	0.3×10^{9}

Table 6 Fuel cost (Rs./hr) and emission (tons/hr) for 15-Unit, 40-Unit, and 140-Unit BFO systems with and without transmission loss

Power demand in (MW)	**Fuel price in rupees per hour and emission in tonnes per hour for 15-unit BFO system without and with transmission loss**	**Fuel price in rupees per hour and emission in tonnes per hour for 40-unit BFO system without and with transmission loss**	**Fuel price in rupees per hour and emission in tonnes per hour for 140-unit BFO system without and with transmission loss**
2580/10303/55984	3310002	202×10^{6}	127×10^{7}
2580/10303/55984	5100003	5800003	0.6×10^{9}
2580/10303/55984	2205004	327×10^{7}	6×10^{9}
2580/10303/55984	3650005	6×10^{6}	0.4×10^{9}

Table 7 Fuel cost (Rs./hr) and emission (tons/hr) for 15-Unit, 40-Unit, and 140-Unit gwo systems with and without transmission loss

Power demand in (MW)	**Fuel price in rupees per hour and emission in tonnes per hour for 15-unit GWO system without and with transmission loss**	**Fuel price in rupees per hour and emission in tonnes per hour for 40-unit GWO system without and with transmission loss**	**Fuel price in rupees per hour and emission in tonnes per hour for 140-unit GWO system without and with transmission loss**
2580/10303/55984	3310003	202×10^{6}	128×10^{7}
2580/10303/55984	5100004	5800003	0.7×10^{9}
2580/10303/55984	2205005	327.5×10^{7}	7×10^{9}
2580/10303/55984	3650006	7×10^{6}	0.5×10^{9}

The optimal overall expense achieved using the proposed vector PSO approach is found to be substantially lower compared to other heuristic methods [54, 55]. Implementing the vector PSO method can lead to significant cost savings, particularly when considering a typical annual operational duration of 7,500 hours. If the observed hourly savings are extrapolated across the year, the vector-based PSO method yields an estimated annual cost reduction of approximately ₹615,000 compared to the WIPSO approach [56], which exhibited the highest operational cost among the methods analyzed.

These substantial cost savings strongly advocate for the implementation of the vector PSO method in power generation systems. The findings highlight its superior economic efficiency in addressing the CEED problem [57]. The following section presents a structured discussion encompassing key findings, interpretation of results, practical implications, potential limitations, and strategic recommendations based on the comparative evaluation of the vector PSO method in the context of CEED.

Scalability analysis of the vector PSO method across varying grid sizes

Examining the performance of the vector PSO method across different grid sizes provides valuable insights into its scalability, adaptability, and optimization efficiency. The following discussion presents a detailed analysis of its behavior and challenges across small to very large grid configurations.

1. Small Grid Sizes (e.g., 5×5 or 10×10): In smaller grid configurations, the vector PSO method tends to exhibit high efficiency and accuracy due to the relatively limited search space. With fewer nodes to evaluate, the algorithm converges quickly, often producing optimal solutions within minimal computational time. However, performance in such cases may be sensitive to the initialization of the particle swarm and the choice of key parameters such as inertia weight and acceleration coefficients. Fine-tuning these parameters is essential to avoid premature convergence or suboptimal results.
2. Medium Grid Sizes (e.g., 20×20 or 30×30): As the grid size increases, the optimization landscape becomes more complex. While the vector PSO method generally maintains good performance in medium-sized grids, achieving convergence may require more iterations. Careful monitoring of convergence behavior and computational efficiency becomes important, as the demand on memory and processing resources rises. Parameter tuning and appropriate swarm size adjustments can help maintain solution quality and stability.
3. Large Grid Sizes (e.g., 50×50 or 100×100): In larger grid environments, the scalability of the algorithm becomes a more prominent concern. The significantly expanded search space increases the risk of the swarm being trapped in local optima. Without adaptive strategies, the algorithm's performance may degrade in terms of convergence speed and solution accuracy. To address these issues, enhancements such as adaptive parameter control, dynamic swarm resizing, or hybridization with other metaheuristics may be implemented. Additionally, leveraging parallelization techniques can help distribute the computational load and expedite convergence.
4. Very Large Grid Sizes (e.g., 200×200 or larger): Extremely large grid sizes pose substantial challenges to any optimization algorithm. For the vector PSO method, issues such as slow convergence, excessive computational burden, and potential stagnation become critical. In these scenarios, advanced methods such as distributed or multi-swarm PSO, decomposition-based optimization, and hybrid metaheuristic frameworks should be considered. Problem-specific adaptations or hierarchical decomposition strategies may also be necessary to divide the task into manageable sub-problems. These approaches can improve tractability and enhance the algorithm’s robustness in high-dimensional settings.

By systematically evaluating the vector PSO method across different grid sizes, researchers can better understand its scalability characteristics and operational boundaries. Such an analysis not only informs appropriate algorithmic enhancements but also supports its effective deployment across diverse problem domains and scales. The insights gained from this investigation are instrumental in refining the vector PSO method for real-world applications that demand scalable and adaptive optimization solutions.

The vector PSO method demonstrates favorable convergence properties in smaller grid systems; however, its efficiency tends to decline as grid size increases, particularly in scenarios involving multiple conflicting objectives. In multi-objective generation dispatch problems, the vector PSO approach effectively identifies Pareto-optimal solutions, illustrating trade-offs between objectives such as fuel cost minimization and emission reduction.

An analysis of fuel cost and emission level variations with respect to real power—both with and without transmission losses—has been conducted for three test systems comprising 15, 40, and 140 units. These results are presented and discussed under the subsequent subheadings. As grid size expands, the algorithm's computational burden intensifies, leading to diminished optimization performance and slower convergence rates. This highlights the inherent trade-off between computational complexity and solution quality in large-scale systems.

The selection of objective functions significantly influences the algorithm's behavior, often resulting in varied Pareto-optimal frontiers. Sensitivity analysis further reveals that parameter tuning—such as inertia weight, acceleration coefficients, and swarm size—is crucial for achieving optimal performance, especially in large-scale grids.

Despite these challenges, the vector PSO method offers strong practical utility in solving generation dispatch problems, particularly in small to medium-sized networks where it maintains satisfactory convergence and solution quality. By generating diverse Pareto-optimal solutions, the method equips decision-makers with valuable insights into the trade-offs between economic and environmental objectives, thereby facilitating informed and balanced decision-making.

These findings highlight the need for further technological enhancements, including adaptive mechanisms and hybrid frameworks, to improve the scalability and robustness of the vector PSO method for large-scale grid optimization problems.

Limitations

While the vector PSO method demonstrates strong performance in small to medium-sized systems, its scalability is significantly constrained by computational resource demands, limiting its effectiveness in very large grid environments. As the grid size increases, the algorithm tends to suffer from slow convergence or may prematurely settle on suboptimal solutions, reducing the overall optimization quality. Furthermore, the presence of complex, multi-objective functions introduce additional challenges, making it difficult to accurately represent the problem landscape and potentially hindering the algorithm’s effectiveness.

To overcome these limitations, several enhancement strategies have been proposed. Parameter optimization plays a critical role in tailoring the algorithm to different problem scales and objective functions, thereby improving convergence behavior and solution accuracy. Hybridization with other metaheuristic approaches, such as GA or simulated annealing, can be explored to enhance scalability and prevent premature convergence. Additionally, the use of parallelization techniques enables the distribution of computational workload, significantly accelerating convergence, especially in large-scale systems. Problem decomposition strategies further support scalability by dividing complex optimization tasks into smaller, manageable sub-problems, facilitating more efficient computation and solution generation in extensive grid systems.

Emission reduction

The vector PSO technique has proven to be highly effective in reducing emissions while simultaneously achieving substantial cost savings. In light of increasing regulatory and environmental constraints, emission control is becoming an essential component of electricity generation. The comparative results of this study indicate that, relative to other heuristic methods such as WIPSO, BFO, and GWO, the vector PSO technique results in cost savings of approximately ₹615,000, ₹123,000, and ₹184,500 per hour, respectively. These findings not only highlight the method's economic benefits but also reinforce its environmental significance, demonstrating that the vector PSO technique can achieve significant emission reductions at minimal additional cost.

Convergence and Reliability

The vector PSO method further distinguishes itself through superior convergence behavior and high reliability. Compared to other algorithms, it exhibits a notably smaller average deviation across multiple trials, reflecting stable performance and precise optimization. The narrow range and lower average fuel costs obtained consistently during repeated simulations indicate the robustness and dependability of the proposed approach. Moreover, the algorithm’s consistent ability to identify the optimal solution reinforces its reliability, which is critical for real-world power generation systems. Reliable optimization ensures continuous, efficient operation and long-term economic performance, making the vector PSO method a dependable tool for dispatch planning.

Operational performance

The vector PSO approach presents a highly effective and economically viable solution for enhancing fuel efficiency and reducing emissions in power generation systems. The study confirms that this method outperforms other heuristic techniques such as WIPSO, BFO, and GWO in terms of both cost optimization and environmental impact. The significant cost savings associated with vector PSO make it an attractive option for power generation facilities aiming to improve financial efficiency. Furthermore, its proven ability to minimize emissions aligns well with environmental regulations and sustainability goals, thereby promoting greener energy production practices. The findings of this investigation clearly demonstrate the dual advantage of the vector PSO technique in optimizing both operational and environmental performance. For power plants, it offers a cost-effective strategy to enhance overall efficiency. Future research may further investigate the underlying mechanisms contributing to the superior performance of vector PSO and explore its adaptability across diverse power generation scenarios under varying operational constraints.

Performance characteristics

The various performance attributes of the proposed approach are presented below, reinforcing the validity of the research findings. The variation in fuel cost and emission levels with respect to real power, both with and without transmission loss, has been illustrated for different system sizes. For the 15-unit system, the results are depicted in *Figures 3, 4, 5*, and *6;* for the 40-unit system, in *Figures 7, 8, 9*, and *10*; and for the 140-unit system, in *Figures 11, 12, 13*, and *14*. These visual representations effectively demonstrate the behavior and performance of the vector PSO method across varying system scales under different operational conditions. A complete list of abbreviations is listed in *Appendix I.*

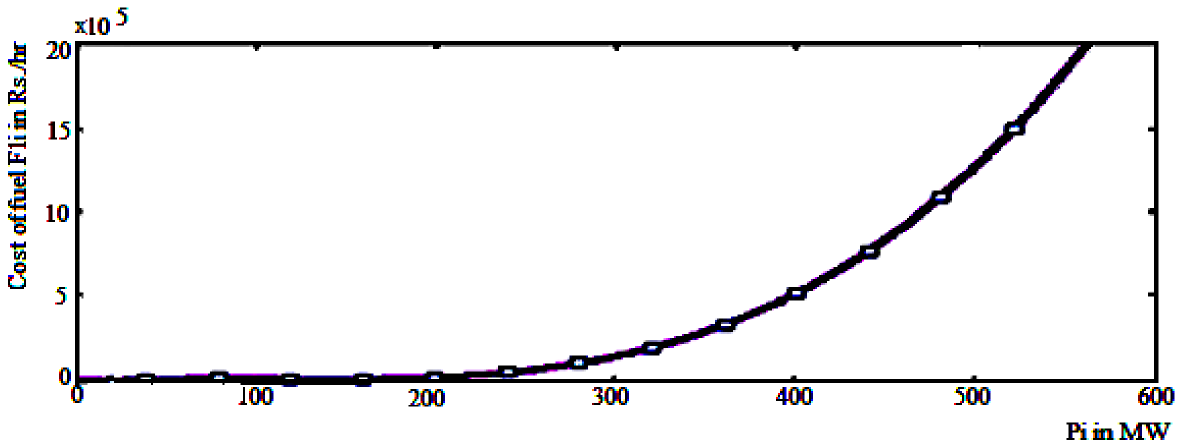

Figure 3 Variation of generation cost vs. real power without transmission loss for IEEE 15-Unit system

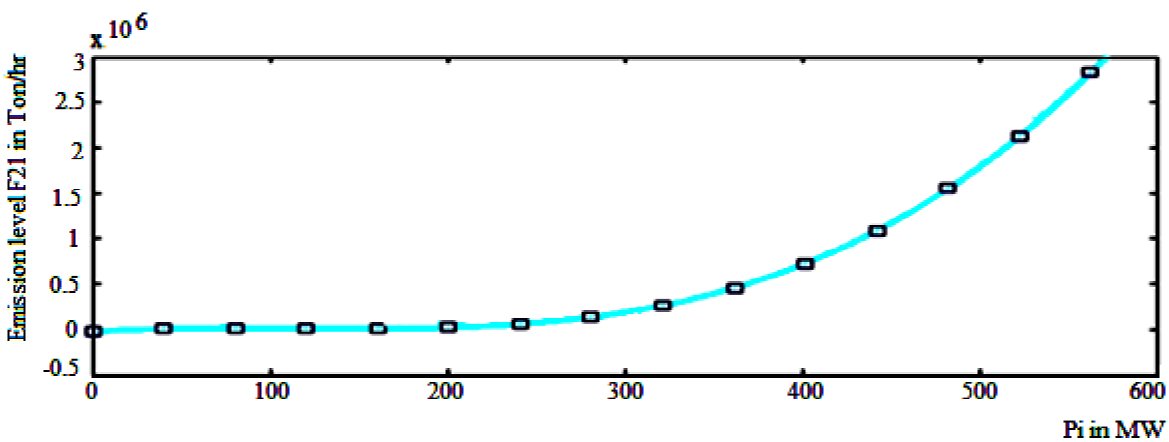

Figure 4 Variation of emission level (tons/hr) vs. real power without transmission loss for IEEE 15-Unit system

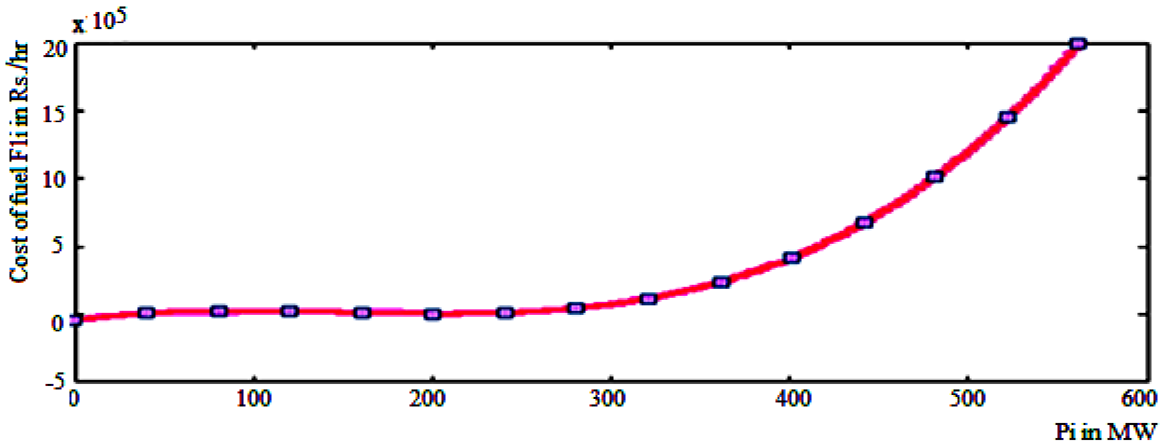

Figure 5 Variation of generation cost vs. real power with transmission loss for IEEE 15-Unit system

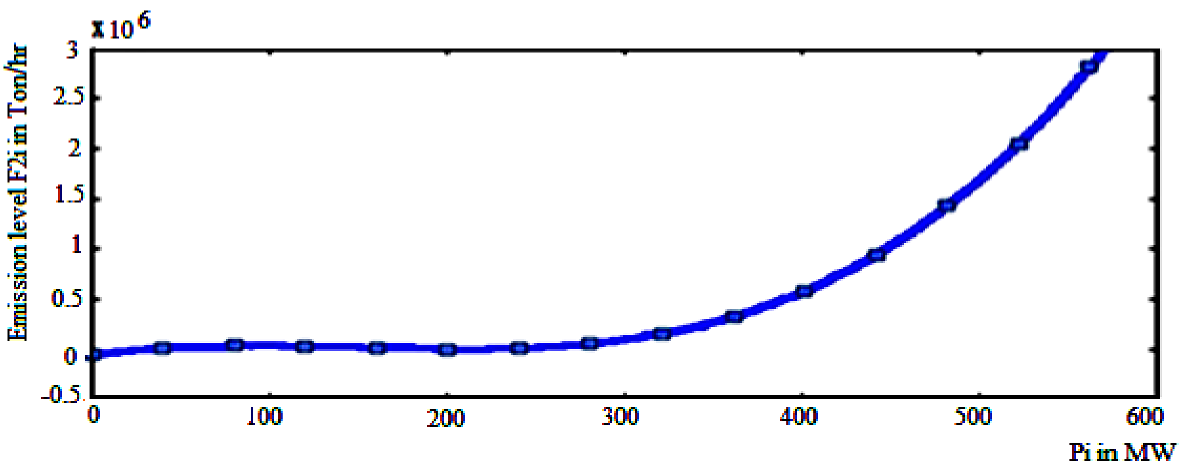

Figure 6 Variation of emission level (tons/hr) versus real power with transmission loss for the IEEE 15-Unit system

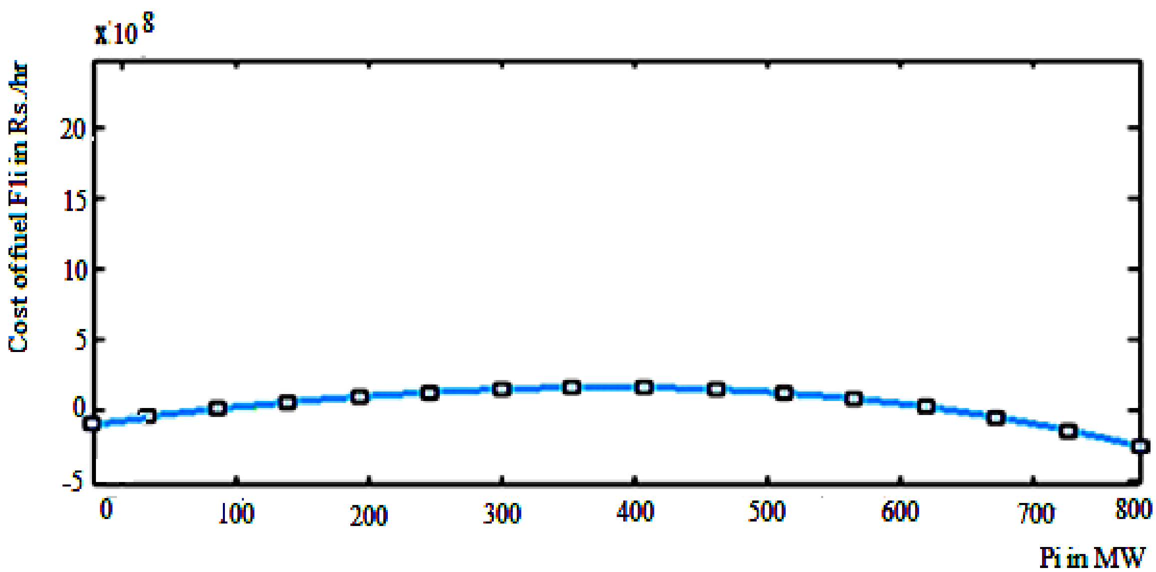

Figure 7 Variation of cost of generation versus real power without transmission loss for the IEEE 40-Unit system

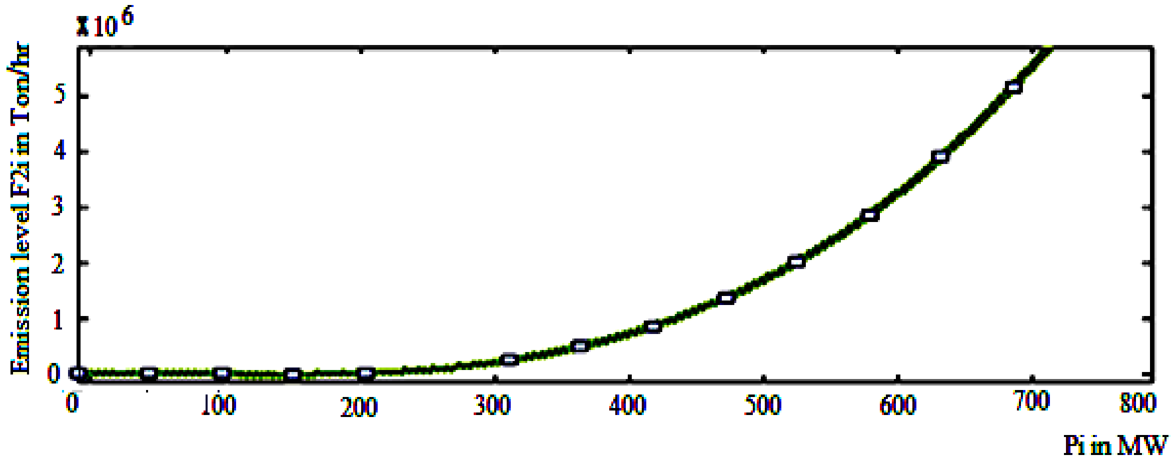

Figure 8 Variation of emission level (ton/hr) versus real power without transmission loss for the IEEE 40-Unit system

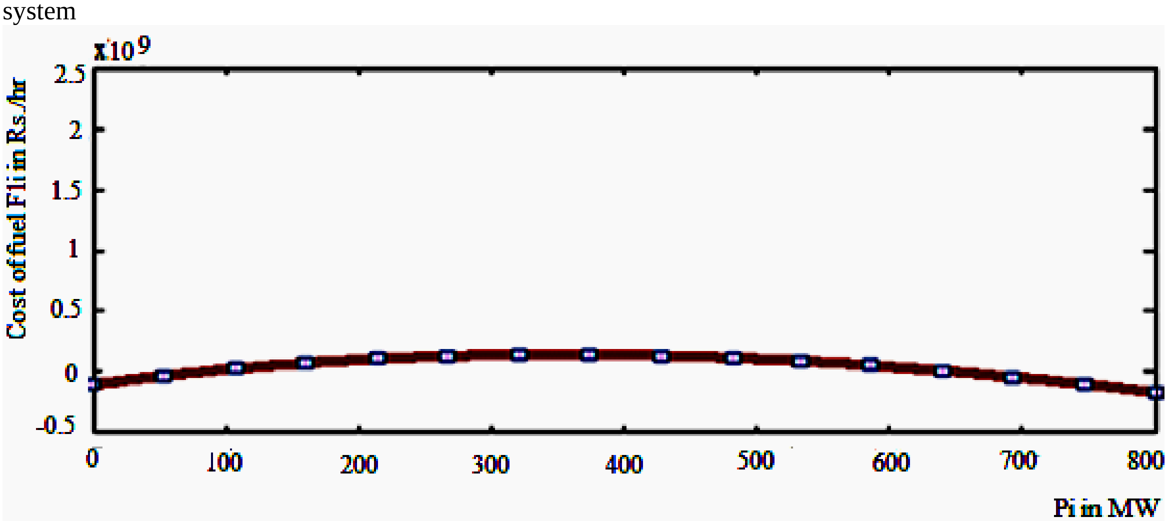

Figure 9 Variation of cost of generation versus real power with transmission loss for the IEEE 40-Unit system

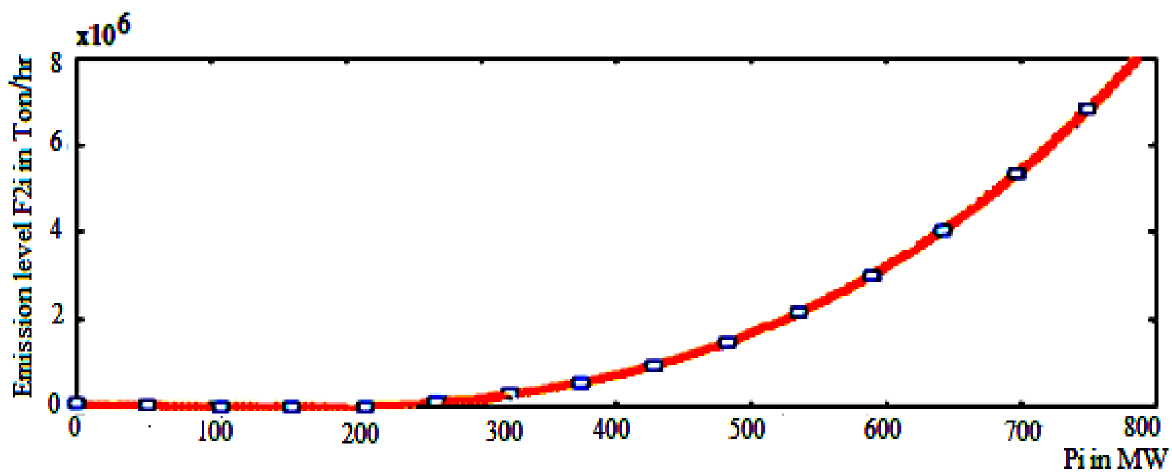

Figure 10 Variation of emission level (ton/hr) versus real power with transmission loss for the IEEE 40-Unit system

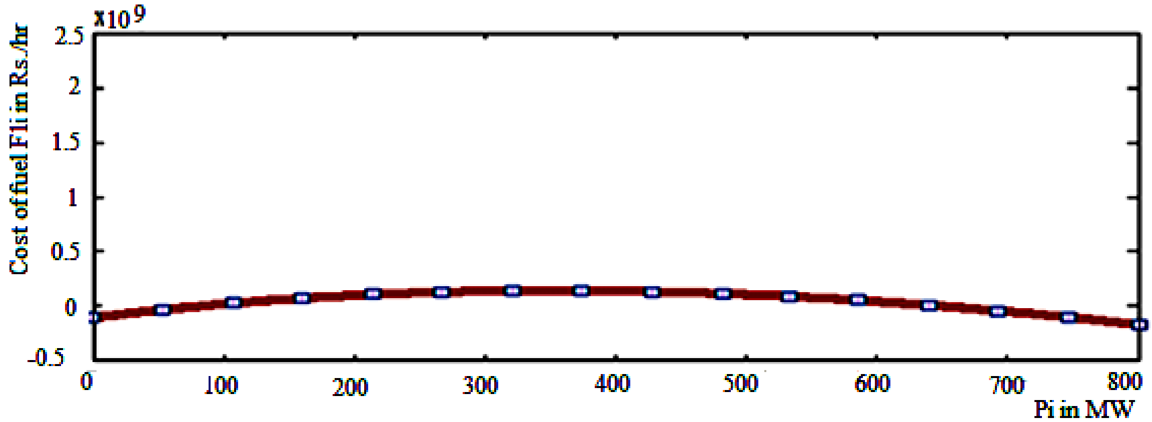

Figure 11 Variation of cost of generation versus real power without transmission loss for the IEEE 140-Unit system

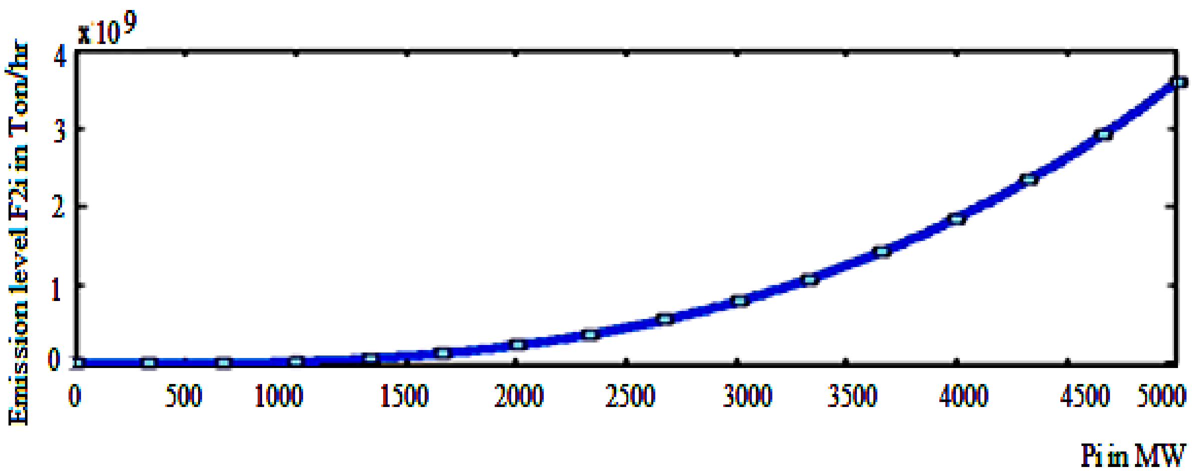

Figure 12 Variation of emission level (ton/hr) versus real power without transmission loss for the IEEE 140-Unit system

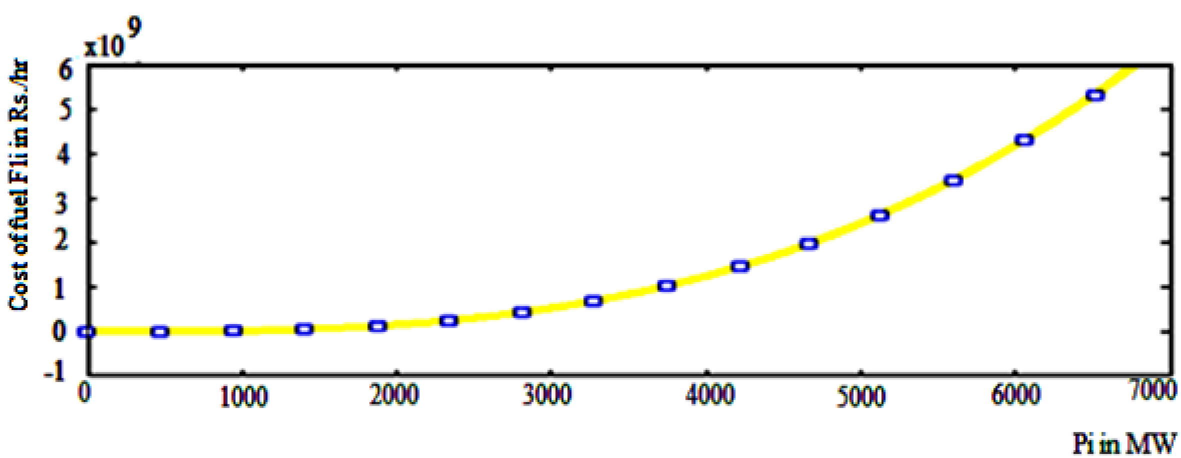

Figure 13 Variation of cost of generation versus real power with transmission loss for the IEEE 140-Unit system

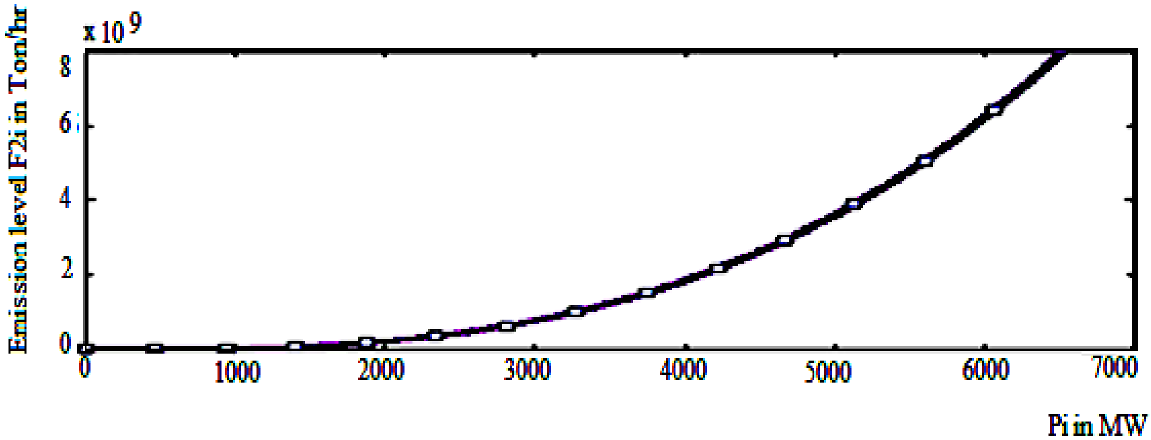

Figure 14 Variation of emission level (ton/hr) versus real power with transmission loss for the IEEE 140-Unit system

5.Conclusion

This study presents an advanced optimization framework based on EVPSO to address the complex challenges of CEED in modern power systems. By integrating electromagnetic principles into the conventional PSO structure, the proposed method effectively enhances exploration and exploitation balance, mitigates premature convergence, and delivers consistent, high-quality solutions across multiple test systems of varying scales—15, 40, and 140 generating units. The optimization model incorporates practical constraints such as valve point effects, ramp rate limits, and transmission losses, accurately reflecting real-world operational conditions. Comparative simulations against state-of-the-art metaheuristic algorithms such as WIPSO, BFO, and GWO demonstrate the superior performance of EVPSO in minimizing both fuel cost and emission levels. Notably, EVPSO achieves significant economic benefits, yielding an estimated annual savings of approximately ₹615,000 compared to WIPSO, and simultaneously ensures regulatory compliance by reducing pollutant emissions. The technique also shows robust convergence behavior and reduced deviation across multiple trials, underscoring its reliability and operational stability. Moreover, the scalability analysis reveals that EVPSO maintains high efficiency in small- to medium-scale systems, with performance gradually tapering in very large grids due to increased computational complexity. These findings highlight the importance of hybridization and adaptive enhancements for future scalability improvements. The proposed EVPSO algorithm offers a powerful, adaptable, and environmentally responsible solution for economic dispatch in modern power systems. Its ability to handle nonlinearities, multiple objectives, and operational constraints positions it as a compelling tool for next-generation smart grid optimization. Future work may focus on real-time deployment, integration with renewable sources, and further hybridization to extend its applicability to broader, more dynamic energy systems.

Acknowledgment

The authors gratefully acknowledge GITA Autonomous College for providing the necessary resources and support in the preparation of this research paper.

Conflicts of interest

The authors have no conflicts of interest to declare.

Data availability

The data used in this study is not publicly available. However, it can be provided by the corresponding author upon reasonable request.

Author’s contribution statement

Nilanjan Mitra: Conceptualization, investigation, writing – original draft, writing – review and editing. **Saroja Kumar Dash:** Data collection, conceptualization, writing – original draft, analysis and interpretation of results**. Himanshu Shekhar Maharana:** Study conception, design, data collection, investigation on challenges and draft manuscript preparation.

References

[1] Han F, Chen WT, Ling QH, Han H. Multi-objective particle swarm optimization with adaptive strategies for feature selection. Swarm and Evolutionary Computation. 2021; 62:100847.

[2] Niknam T, Azizipanah-abarghooee R, Aghaei J. A new modified teaching-learning algorithm for reserve constrained dynamic economic dispatch. IEEE Transactions on Power Systems. 2012; 28(2):749-63.

[3] Fard AK, Akbari-zadeh MR. A hybrid method based on wavelet, ANN and ARIMA model for short-term load forecasting. Journal of Experimental & Theoretical Artificial Intelligence. 2014; 26(2):167-82.

[4] Bhattacharjee K, Bhattacharya A, Nee DSH. Solution of economic emission load dispatch problems of power systems by real coded chemical reaction algorithm. International Journal of Electrical Power & Energy Systems. 2014; 59:176-87.

[5] Rajasomashekar S, Aravindhababu P. Biogeography based optimization technique for best compromise solution of economic emission dispatch. Swarm and Evolutionary Computation. 2012; 7:47-57.

[6] Yang HT, Yang PC, Huang CL. Evolutionary programming based economic dispatch for units with non-smooth fuel cost functions. IEEE Transactions on Power Systems. 1996; 11(1):112-8.

[7] Sinha N, Chakrabarti R, Chattopadhyay PK. Evolutionary programming techniques for economic load dispatch. IEEE Transactions on Evolutionary Computation. 2003; 7(1):83-94.

[8] Kavousi-fard A, Niknam T. Optimal distribution feeder reconfiguration for reliability improvement considering uncertainty. IEEE Transactions on Power Delivery. 2013; 29(3):1344-53.

[9] Alsumait JS, Sykulski JK, Al-othman AK. A hybrid GA–PS–SQP method to solve power system valve-point economic dispatch problems. Applied Energy. 2010; 87(5):1773-81.

[10] Clerc M. The swarm and the queen: towards a deterministic and adaptive particle swarm optimization. In proceedings of the congress on evolutionary computation-CEC99 (Cat. No. 99TH8406) 1999 (pp. 1951-7). IEEE.

[11] Eberhart R, Kennedy J. A new optimizer using particle swarm theory. In MHS'95. proceedings of the sixth international symposium on micro machine and human science 1995 (pp. 39-43). IEEE.

[12] Fan SK, Zahara E. A hybrid simplex search and particle swarm optimization for unconstrained optimization. European Journal of Operational Research. 2007; 181(2):527-48.

[13] Ho SL, Yang SY, Ni GZ, Wong KF. An improved PSO method with application to multimodal functions of inverse problems. IEEE Transactions on Magnetics. 2007; 43(4):1597-600.

[14] Shi Y, Eberhart R. A modified particle swarm optimizer. In international conference on evolutionary computation proceedings. IEEE world congress on computational intelligence (Cat. No. 98TH8360) 1998 (pp. 69-73). IEEE.

[15] Li-ping Z, Huan-jun Y, Shang-xu H. Optimal choice of parameters for particle swarm optimization. Journal of Zhejiang University-Science A. 2005; 6(6):528-34.

[16] Amjady N, Sharifzadeh H. Solution of non-convex economic dispatch problem considering valve loading effect by a new modified differential evolution algorithm. International Journal of Electrical Power & Energy Systems. 2010; 32(8):893-903.

[17] Niknam T, Mojarrad HD, Meymand HZ. A novel hybrid particle swarm optimization for economic dispatch with valve-point loading effects. Energy Conversion and Management. 2011; 52(4):1800-9.

[18] Kumar R, Sharma D, Sadu A. A hybrid multi-agent based particle swarm optimization algorithm for economic power dispatch. International Journal of Electrical Power & Energy Systems. 2011; 33(1):115-23.

[19] Subbaraj P, Rengaraj R, Salivahanan S, Senthilkumar TR. Parallel particle swarm optimization with modified stochastic acceleration factors for solving large scale economic dispatch problem. International Journal of Electrical Power & Energy Systems. 2010; 32(9):1014-23.

[20] Gao H, Xu W. A new particle swarm algorithm and its globally convergent modifications. IEEE Transactions on Systems, Man, and Cybernetics, Part B (Cybernetics). 2011; 41(5):1334-51.

[21] Nickabadi A, Ebadzadeh MM, Safabakhsh R. A novel particle swarm optimization algorithm with adaptive inertia weight. Applied Soft Computing. 2011; 11(4):3658-70.

[22] Ghasemi M, Aghaei J, Akbari E, Ghavidel S, Li L. A differential evolution particle swarm optimizer for various types of multi-area economic dispatch problems. Energy. 2016; 107:182-95.

[23] Mason K, Duggan J, Howley E. Multi-objective dynamic economic emission dispatch using particle swarm optimisation variants. Neurocomputing. 2017; 270:188-97.

[24] Kaur P, Chaturvedi KT, Kolhe ML. Economic dispatch of combined heat and power plant units within energy network integrated with wind power plant. Processes. 2023; 11(4):1-17.

[25] Lim WH, Isa NA. Particle swarm optimization with adaptive time-varying topology connectivity. Applied Soft Computing. 2014; 24:623-42.

[26] Liu B, Wang L, Jin YH, Tang F, Huang DX. Improved particle swarm optimization combined with chaos. Chaos, Solitons & Fractals. 2005; 25(5):1261-71.

[27] Kaucic M. A multi-start opposition-based particle swarm optimization algorithm with adaptive velocity for bound constrained global optimization. Journal of Global Optimization. 2013; 55:165-88.

[28] Fu X, Chan FT, Niu B, Chung NS, Qu T. A three-level particle swarm optimization with variable neighbourhood search algorithm for the production scheduling problem with mould maintenance. Swarm and Evolutionary Computation. 2019; 50:100572.

[29] Habib S, Kamarposhti MA, Shokouhandeh H, Colak I, Barhoumi EM. Economic dispatch optimization considering operation cost and environmental constraints using the HBMO method. Energy Reports. 2023; 10:1718-25.

[30] Aras S, Gedikli E, Kahraman HT. A novel stochastic fractal search algorithm with fitness-distance balance for global numerical optimization. Swarm and Evolutionary Computation. 2021; 61:100821.
[31] Han H, Bai X, Han H, Hou Y, Qiao J. Self-adjusting multitask particle swarm optimization. IEEE Transactions on Evolutionary Computation. 2021; 26(1):145-58.
[32] Bhargava G, Yadav NK. Solving combined economic emission dispatch model via hybrid differential evaluation and crow search algorithm. Evolutionary Intelligence. 2022; 15(2):1161-9.
[33] Pehlivanoglu YV. A new particle swarm optimization method enhanced with a periodic mutation strategy and neural networks. IEEE Transactions on Evolutionary Computation. 2012; 17(3):436-52.
[34] Qin Q, Cheng S, Zhang Q, Li L, Shi Y. Biomimicry of parasitic behavior in a coevolutionary particle swarm optimization algorithm for global optimization. Applied Soft Computing. 2015; 32:224-40.
[35] Cheng R, Jin Y. A social learning particle swarm optimization algorithm for scalable optimization. Information Sciences. 2015; 291:43-60.
[36] Tang D, Cai Y, Zhao J, Xue Y. A quantum-behaved particle swarm optimization with memetic algorithm and memory for continuous non-linear large scale problems. Information Sciences. 2014; 289:162-89.
[37] Hota PK, Sahu NC. Non-convex economic dispatch with prohibited operating zones through gravitational search algorithm. International Journal of Electrical and Computer Engineering. 2015; 5(6):1234-44.
[38] Giri SK, Mohan A, Sharma AK. Economic load dispatch in power system by hybrid swarm intelligence. International Journal of Recent Technology and Engineering. 2019; 8:1584-92.
[39] Chapa MG, Galaz JV. An economic dispatch algorithm for cogeneration systems. In IEEE power engineering society general meeting, 2004 (pp. 989-94). IEEE.
[40] Rao PN. Combined heat and power economic dispatch: a direct solution. Electric Power Components and Systems. 2006; 34(9):1043-56.
[41] Almalaq A, Guesmi T, Albadran S. A hybrid chaotic-based multiobjective differential evolution technique for economic emission dispatch problem. Energies. 2023; 16(12):1-34.
[42] Ouyang HB, Gao LQ, Li S, Kong XY. Improved global-best-guided particle swarm optimization with learning operation for global optimization problems. Applied Soft Computing. 2017; 52:987-1008.
[43] Kavousi-fard A, Abunasri A, Zare A, Hoseinzadeh R. Impact of plug-in hybrid electric vehicles charging demand on the optimal energy management of renewable micro-grids. Energy. 2014; 78:904-15.
[44] Qu BY, Suganthan PN, Das S. A distance-based locally informed particle swarm model for multimodal optimization. IEEE Transactions on Evolutionary Computation. 2012; 17(3):387-402.
[45] Verma P, Parouha RP. An innovative hybrid algorithm for solving combined economic and emission dispatch problems. Soft Computing. 2022; 26(22):12635-66.
[46] Hassan MH, Yousri D, Kamel S, Rahmann C. A modified Marine predators algorithm for solving single-and multi-objective combined economic emission dispatch problems. Computers & Industrial Engineering. 2022; 164:107906.
[47] Wang H, Yang S, Ip WH, Wang D. A memetic particle swarm optimisation algorithm for dynamic multi-modal optimisation problems. International Journal of Systems Science. 2012; 43(7):1268-83.
[48] Guan Y, Wei B, Guerrero JM, Vasquez JC, Gui Y. An overview of the operation architectures and energy management system for multiple microgrid clusters. iEnergy. 2022; 1(3):306-14.
[49] Kim HJ, Kim MK. A novel deep learning-based forecasting model optimized by heuristic algorithm for energy management of microgrid. Applied Energy. 2023; 332:120525.
[50] Kaur P, Chaturvedi KT, Kolhe ML. Techno-economic power dispatching of combined heat and power plant considering prohibited operating zones and valve point loading. Processes. 2022; 10(5):1-17.
[51] Kaur P, Chaturvedi KT, Kolhe ML. Combined heat and power economic dispatching within energy network using hybrid metaheuristic technique. Energies. 2023; 16(3):1-17.
[52] Qiao J, Wang G, Yang Z, Luo X, Chen J, Li K, et al. A hybrid particle swarm optimization algorithm for solving engineering problem. Scientific Reports. 2024; 14(1):1-30.
[53] Mishra A, Tripathy M, Ray P. A survey on different techniques for distribution network reconfiguration. Journal of Engineering Research. 2024; 12(1):173-81.
[54] Ozkaya B, Kahraman HT, Duman S, Guvenc U, Akbel M. Combined heat and power economic emission dispatch using dynamic switched crowding based multi-objective symbiotic organism search algorithm. Applied Soft Computing. 2024; 151:111106.
[55] Yuan ZP, Li P, Li ZL, Xia J. A fully distributed privacy-preserving energy management system for networked microgrid cluster based on homomorphic encryption. IEEE Transactions on Smart Grid. 2023; 15(2):1735-48.
[56] Lin W, Zhang B, Lu R. A novel hybrid deep learning model for photovoltaic power forecasting based on feature extraction and bilstm. IEEJ Transactions on Electrical and Electronic Engineering. 2024; 19(3):305-17.
[57] Ozkaya B, Duman S, Kahraman HT, Guvenc U. Optimal solution of the combined heat and power economic dispatch problem by adaptive fitness-distance balance based artificial rabbits optimization algorithm. Expert Systems with Applications. 2024; 238:122272.

Nilanjan Mitra is currently pursuing the final year of his M.Tech degree at GITA Autonomous College, Bhubaneswar, under Biju Patnaik University of Technology (BPUT), Odisha, India. He completed his B.Tech from Birbhum Institute of Engineering and Technology, affiliated with West Bengal University of Technology (WBUT), Kolkata
Email: wapcosmitra@gmail.com

Dr. Saroja Kumar Dash received his Bachelor's degree in Electrical Engineering from The Institution of Engineers (India) in 1991, followed by a Master's degree from VSSUT (formerly SU), Odisha, in 1998. He completed his Ph.D. at Utkal University, Odisha, India, in 2006. He is currently serving as Professor and Head of the Department of Electrical Engineering at GITA Autonomous College, Bhubaneswar, affiliated with Biju Patnaik University of Technology (BPUT), Odisha. Dr. Dash has received notable accolades including the Pandit Madan Mohan Malaviya Award, the Union Ministry of Power Prize, and multiple gold medals for his research contributions on "Economic Load Dispatching of Power Plants with Multi-Fuel Options" and "Short-Term Generation Scheduling with Take-or-Pay Fuel Contracts Using Evolutionary Algorithms.
Email: hodeegita@gmail.com

Himanshu Shekhar Maharana completed his B.Tech in Electrical and Electronics Engineering from JITM, Paralakhemundi, under Biju Patnaik University of Technology (BPUT), Odisha, in 2010. He earned his M.Tech in Power System Engineering from GITA, Bhubaneswar (also under BPUT), in 2014. Prior to his doctoral studies, he gained experience in Java Full-Stack Software Development using online teaching models. Currently, he is pursuing a full-time Ph.D. in Electrical Engineering at GITA Autonomous College, Bhubaneswar. His research focuses on Power System Engineering and the application of Optimization Techniques in Economic Load Dispatch for electric power systems.
Email: hsmaharana@gmail.com

Appendix I

S. No.	Abbreviation	Description
1	ANN	Artificial Neural Network
2	ARIMA	Autoregressive Integrated Moving Average
3	BBO	Biogeography-Based Optimization
4	BFO	Bacterial Foraging Optimization
5	CEED	Combined Economic and Emission Dispatch
6	CO_2	Carbon Dioxide
7	DE	Differential Evolution
8	DEED	Dynamic Economic Emission Dispatch
9	ELD	Economic Load Dispatch
10	EP	Evolutionary Programming
11	EVPSO	Electromagnetic Vector Particle Swarm Optimization
12	GA	Genetic Algorithm
13	GWO	Gray Wolf Optimization
14	HBMO	Honey Bee Mating Optimization
15	MSSA	Multi-Objective Simulated Annealing Local Search Pattern Swarm Algorithm
16	N_2O	Nitrous Oxide
17	PSO	Particle Swarm Optimization
18	SALP	Simulated Annealing Local Search Pattern
19	SO_2	Sulfur Dioxide
20	VPL	Valve Point Loading
21	VPSO	Vector Particle Swarm Optimization
22	WIPSO	Weight Improved Particle Swarm Optimization